Advanced Drug Delivery Reviews 99 (2016) 12–27

Contents lists available at ScienceDirect

Advanced Drug Delivery Reviews

journal homepage: www.elsevier.com/locate/addr

Targeted delivery to bone and mineral deposits using bisphosphonate ligands☆,☆☆

Lisa E. Cole [a,c], Tracy Vargo-Gogola [b,c], Ryan K. Roeder [a,c,*]

[a] Department of Aerospace and Mechanical Engineering, Bioengineering Graduate Program, University of Notre Dame, Notre Dame, IN 46556, United States
[b] Department of Biochemistry and Molecular Biology, Indiana University Simon Cancer Center, Indiana University School of Medicine-South Bend, South Bend, IN 46617, United States
[c] Harper Cancer Research Institute, University of Notre Dame, Notre Dame, IN 46556, United States

ARTICLE INFO

Article history:
Received 25 June 2015
Received in revised form 1 October 2015
Accepted 9 October 2015
Available online 19 October 2015

Keywords:
Bisphosphonate
Bone
Calcifications
Drug Delivery
Hydroxyapatite
Diagnostic imaging
Radiotherapy
Targeted delivery

ABSTRACT

The high concentration of mineral present in bone and pathological calcifications is unique compared with all other tissues and thus provides opportunity for targeted delivery of pharmaceutical drugs, including radiosensitizers and imaging probes. Targeted delivery enables accumulation of a high local dose of a therapeutic or imaging contrast agent to diseased bone or pathological calcifications. Bisphosphonates (BPs) are the most widely utilized bone-targeting ligand due to exhibiting high binding affinity to hydroxyapatite mineral. BPs can be conjugated to an agent that would otherwise have little or no affinity for the sites of interest. This article summarizes the current state of knowledge and practice for the use of BPs as ligands for targeted delivery to bone and mineral deposits. The clinical history of BPs is briefly summarized to emphasize the success of these molecules as therapeutics for metabolic bone diseases. Mechanisms of binding and the relative binding affinity of various BPs to bone mineral are introduced, including common methods for measuring binding affinity *in vitro* and *in vivo*. Current research is highlighted for the use of BP ligands for targeted delivery of BP conjugates in various applications, including (1) therapeutic drug delivery for metabolic bone diseases, bone cancer, other bone diseases, and engineered drug delivery platforms; (2) imaging probes for scintigraphy, fluorescence, positron emission tomography, magnetic resonance imaging, and computed tomography; and (3) radiotherapy. Last, and perhaps most importantly, key structure–function relationships are considered for the design of drugs with BP ligands, including the tether length between the BP and drug, the size of the drug, the number of BP ligands per drug, cleavable tethers between the BP and drug, and conjugation schemes.

Contents

☆ This review is part of the *Advanced Drug Delivery Reviews* theme issue on "Non-Antigenic Regulators-Maiseyeu".

☆☆ Funding sources: National Science Foundation (DMR-1309587); St. Joseph Regional Medical Center; Walther Cancer Foundation

* Corresponding author at: Department of Aerospace and Mechanical Engineering, Bioengineering Graduate Program, 148 Multidisciplinary Research Building, University of Notre Dame, Notre Dame, IN 46556. Tel.: +1 574 631 7003.
E-mail address: rroeder@nd.edu (R.K. Roeder).

http://dx.doi.org/10.1016/j.addr.2015.10.005
0169-409X/

1. Introduction

Bone pathologies and pathological calcifications in soft tissues can be diagnosed and treated by targeted delivery of imaging probes and pharmaceuticals to these mineral sites. Metabolic bone diseases are characterized by an increase in bone resorption resulting in an imbalance between bone formation and resorption [1]. These diseases include osteoporosis, Paget's disease, bone cancers or metastases, and osteomalacia. The imbalance between bone formation and resorption results in undesired effects such as bone loss, enlarged or weak bones, and fractures [1]. Pathological calcifications are deposits of mineral in soft tissues, such as arterial calcifications in atherosclerosis [2–4], microcalcifications in breast tissue [5], and kidney stones [6]. These abnormal mineral deposits can cause pain, tissue malfunction, and possibly even death if not detected and treated.

The high concentration of mineral present in bone and pathological calcifications is distinct compared with all other tissues and thus provides opportunity for targeted delivery of drugs, including radiosensitizers and imaging probes. Targeted delivery enables the specific accumulation of a high local concentration of a therapeutic or imaging contrast agent to diseased bone or pathological calcifications. One approach to target agents with little or no affinity for bone or mineral deposits is to conjugate the agent to a mineral-binding molecule. Bisphosphonates (BPs) are the most widely utilized bone-binding ligand due to exhibiting high binding affinity to hydroxyapatite mineral. The high binding affinity of BPs for hydroxyapatite is a well-established property of BPs that was discovered in the 1960s and has led to the widespread use of BPs as drugs to treat metabolic bone disorders [7].

The overall goal of this review is to summarize the current state of knowledge and practice for the use of BPs as ligands for targeted delivery to bone and mineral deposits (Fig. 1). The clinical history of BPs is first summarized to highlight the success of these molecules as drugs for metabolic bone diseases, due to the high binding affinity between BPs and bone mineral. Mechanisms of binding and the relative binding affinity of various BPs to bone mineral are introduced, including common methods for measuring binding affinity *in vitro* and *in vivo*. Current research is highlighted for the use of BP ligands for targeted delivery in various applications, including therapeutic drug delivery, imaging probes, and radiotherapy (Fig. 1). Last, and perhaps most importantly, key structure–function relationships are considered for the design of drugs with BP ligands, including the tether length between the BP and drug, the size of the drug, the number of BP ligands per drug, cleavable tethers between the BP and drug, and conjugation schemes.

2. History of bisphosphonates

BPs are a class of molecules used clinically to treat metabolic bone diseases by inhibiting the process of bone resorption. The first evidence for the biological function of BPs was reported by Fleisch and colleagues in 1968 [8]. Inorganic pyrophosphate (Fig. 2) was discovered to inhibit the formation and dissolution of calcium phosphonate crystals [9], suggesting that pyrophosphate regulates bone resorption and formation.

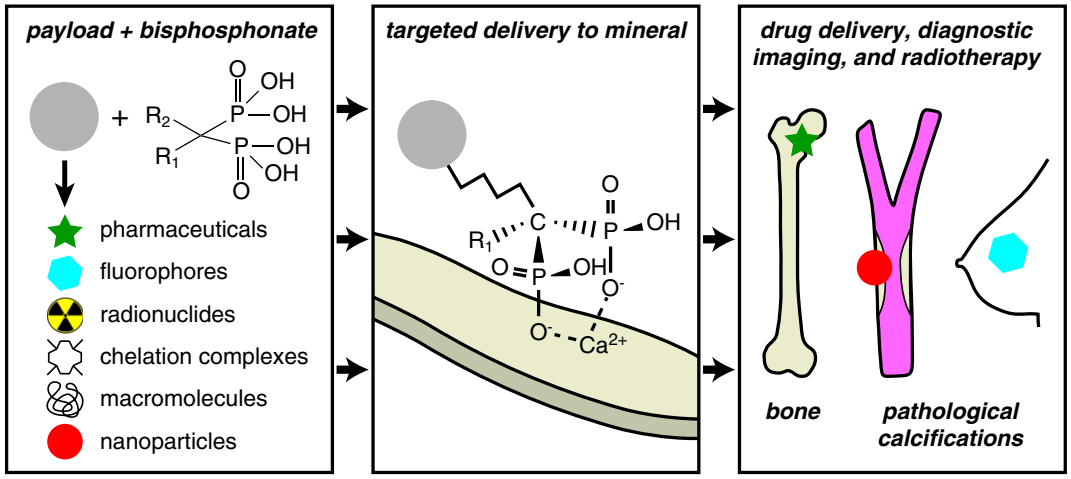

Fig. 1. Schematic diagram showing the use of bisphosphonates, either alone or conjugated to various pharmaceuticals, fluorophores, radionuclides, chelation complexes, macromolecules, and nanoparticles, for targeting mineral in bone and pathological calcifications for drug delivery, diagnostic imaging, and radiotherapy.

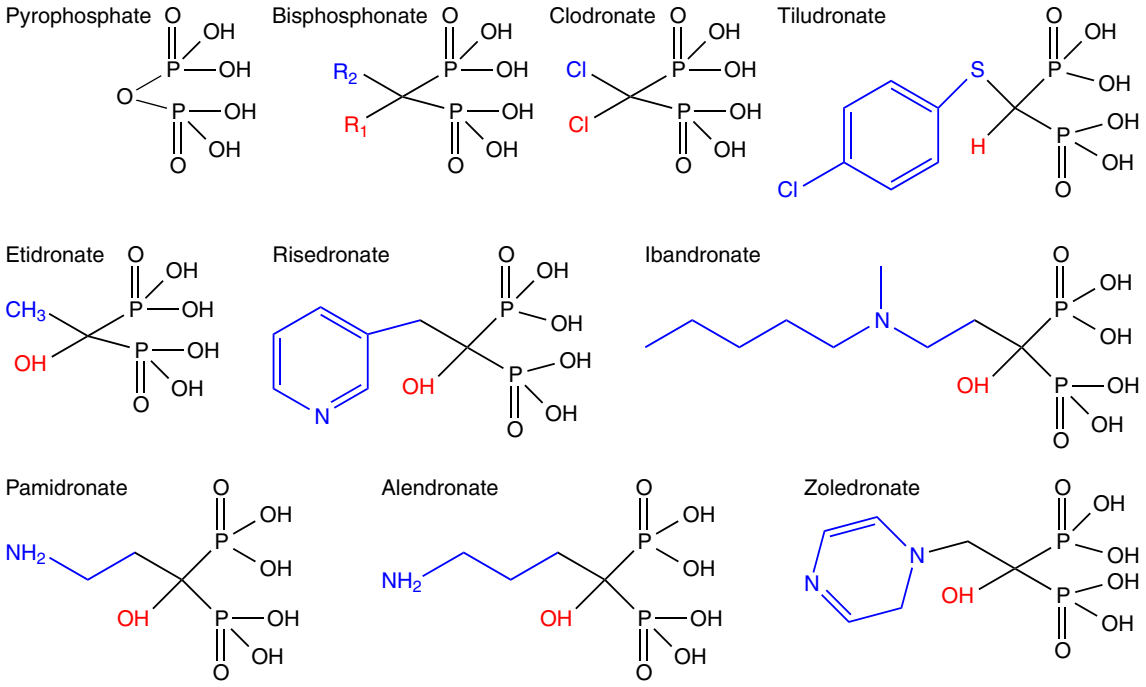

Fig. 2. Molecular structure of pyrophosphate and bisphosphonates, including the seven BPs that are approved for clinical use by the U.S. Food and Drug Administration. Differences in binding affinity (Table 1) and biological activity are primarily governed by the R_1 (red) and R_2 (blue) side groups.

BPs were subsequently synthesized as a more chemically stable analog of pyrophosphate, where the oxygen molecule bound to the two phosphonate molecules in pyrophosphate (P–O–P) was replaced by a carbon (P–C–P) (Fig. 2). This elemental substitution resulted in bonds that were resistant to degradation, creating biologically active molecules that were similar in structure to pyrophosphate and capable of being delivered to bone *in vivo* without degradation by hydrolysis [10]. The first synthesized BPs (sodium dichloromethylene diphosphonate, sodium methylene diphosphonate, and sodium ethane-1-hydroxy-1,1-diphosphonate) were shown to significantly impair *in vivo* bone resorption in rats [10–12], which sparked interest in exploring BP compounds as therapeutics for bone diseases.

A BP therapeutic was first used in humans to inhibit undesired calcification. In 1969, etidronate (Fig. 2) was given to a child with fibrodysplasia ossificans progressiva to treat ectopic calcification [13]. Etidronate was also used to treat ectopic calcifications after spinal cord injury or total hip replacement [8]. However, the efficacy of etidronate in these cases has been inconclusive, perhaps due to the relatively lower binding affinity of etidronate discussed below. Additionally, the dose required to inhibit pathological calcifications in humans, such as kidney stones, was found to also impact normal mineralization [14]. Therefore, etidronate was abandoned for use as an inhibitor of ectopic calcification [8]. The next clinical use of a BP was a bone-targeting radionuclide for nuclear imaging [15], which was developed in the 1970s and is still used today. Bone scintigraphy is a nuclear imaging technique used to detect areas of high bone turnover associated with stress fractures, Paget's disease lesions, and bone cancers or metastases. A BP molecule is conjugated to a gamma-emitting technetium isotope, such that the radionuclide rapidly accumulates in areas of high bone metabolism after intravascular delivery due to the high binding affinity of BP to bone mineral.

BPs are currently the most widely used therapeutic in the treatment of metabolic bone diseases. BPs were introduced for the treatment of osteoporosis in the 1990s and are now the most commonly prescribed pharmaceutical for the treatment of postmenopausal bone loss with annual sales of millions of dollars [16]. The efficacy of BPs for inhibiting bone resorption is largely due to the ability of BPs to selectively bind to bone mineral [7,17] facilitating uptake by osteoclasts during osteoclastic-mediated bone resorption. BPs inhibit the recruitment and differentiation of osteoclasts, and cause morphological cellular changes and osteoclast apoptosis [7,18–21], leading to reduced bone resorption. The high selectivity of BPs for mineral also results in a low overall cytotoxicity profile [22], which facilitated rapid clinical adoption of these drugs. There are seven BP drugs currently approved for clinical use in the U.S. by the Food and Drug Administration, which differ in the structure of the side groups (R_1 and R_2) (Fig. 2).

3. Bisphosphonate binding to bone and mineral deposits

The structure of both the mineral and the BP has been shown to affect binding affinity and must therefore be considered when choosing the appropriate BP ligand for targeting. The most extensive research has focused solely on the interaction between hydroxyapatite mineral and BPs, due to widespread clinical use of BPs as therapeutics for metabolic bone diseases.

3.1. Effects of mineral type and crystal structure

Bone contains the overwhelming majority of mineral in the human body and is therefore crucial for calcium homeostasis. However, relatively minute amounts of pathological mineral deposits can also be associated with disease and are therefore crucial for diagnosis. The mineral phase of bone is a highly substituted carbonated apatite, which has a chemical and crystal structure similar to hydroxyapatite ($Ca_5(PO_4)_3OH$). Pathological mineral deposits occurring within soft tissues are most commonly composed of hydroxyapatite or calcium oxalate (CaC_2O_4).

BPs exhibit a relatively greater binding affinity to hydroxyapatite compared with other calcium minerals such as calcium oxalate, calcium carbonate, or calcium pyrophosphate [23–26]. This suggests that the chemical binding of BPs is dependent on the crystal structure of the mineral surface, where an increased concentration and the most appropriate spacing of superficial Ca^{2+} on hydroxyapatite surfaces enables a higher binding affinity. This relationship is further evidenced by a

lower binding affinity of BPs for carbonated apatite *versus* pure hydroxyapatite due to the distortion of the crystal structure by the substitutions present in carbonated apatite [11,27]. The high binding affinity of BPs to hydroxyapatite compared with other calcium minerals is important for both targeting or avoiding bone. BPs used to treat metabolic bone diseases leverage selectivity for hydroxyapatite. On the other hand, if BP ligands are intended to deliver therapeutics or imaging probes to mineral deposits other than bone, the majority of the dose may be taken up by bone rather than the desired mineral site. High skeletal uptake of an agent intended to target pathological calcifications may be detrimental for efficient targeting, dosing, and avoiding off-target side-effects. Therefore, additional means may be needed to independently target bone *versus* pathological calcifications. However, pathological calcifications are most commonly found in tissues that are normally without mineral deposits when healthy (*e.g.*, kidneys, aorta, breasts) and sufficiently distanced from bone tissue, such that BP conjugate imaging agents can still be effective in detecting these calcifications in spite of high skeletal uptake.

Hydroxyapatite selectivity may also be clinically useful in mammographic screening for breast cancer by detecting breast microcalcifications. Microcalcifications composed of hydroxyapatite are more commonly associated with cancerous lesions compared with those composed of calcium oxalate, which are nearly always associated with benign lesions [5]. A BP conjugated near-infrared imaging probe demonstrated selectivity for hydroxyapatite microcalcifications over calcium oxalate microcalcifications *in vitro* [28] and *in vivo* in rats [26]. This creates opportunity to reduce or eliminate unnecessary biopsies due to false positive detection of calcium oxalate microcalcifications by screening microcalcifications based on the mineral composition.

3.2. Effects of bisphosphonate molecular structure

The molecular structure of BPs (Fig. 2) greatly affects binding affinity to hydroxyapatite (Fig. 3). The P–C–P backbone presenting two phosphonate groups for chelating calcium ions on hydroxyapatite surfaces in a bidentate structure is critical for binding (Fig. 3). Other similar compounds, such as monophosphates or compounds with P–N–P or P–C–C–P backbones exhibit reduced binding affinity for hydroxyapatite [7]. The R_1 side group (Fig. 2) affects the binding affinity. BPs having an –OH in the R_1 [29] exhibit increased affinity due to the capacity for tridentate binding to hydroxyapatite (Fig. 3) [27].

The R_2 side group was originally thought to only impact the pharmacological activity of BP but recent studies demonstrated effects of the R_2 side groups on binding affinity [11]. The kinetic binding affinity of six different BPs for hydroxyapatite was measured to increase in the following order: clodronate, etidronate, risedronate, ibandronate, alendronate, zoledronate [11]. Thus, BPs with a nitrogen in the R_2 side group (zoledronate, alendronate, ibandronate, risedronate) exhibited a greater binding affinity than the non-nitrogen containing BPs (etidronate and clodronate) (Fig. 2). Molecular modeling has suggested that the nitrogen side groups may directly contribute to the binding affinity *via* hydrogen bonding with hydroxyl groups on hydroxyapatite surfaces (Fig. 3) [27,30]. The binding affinity was influenced by both the angle and distance of the N–H–O bond, with optimal binding occurring at a bond angle ≥125° and a bond distance of 3 Å [27,30]. Based on these 3-D models, the molecular structure of alendronate is most advantageous (132°, 2.7 Å), providing an explanation for the higher binding affinity of alendronate compared with other nitrogen-containing BPs [27,30]. Differences in binding affinity were also explained by changes in the zeta potential of hydroxyapatite surfaces after adsorption of BPs *in vitro*, due to the charge associated with the R_2 side groups at pH 7.4. As BPs with positively charged R_2 side groups (zoledronate, alendronate, ibandronate) bind the mineral surface, the zeta potential of the hydroxyapatite surface shifts to become more positively charged. This attracts the negatively charged phosphonate groups of BPs to bind due to electrostatic attraction and increases the binding capacity on the mineral surface [27].

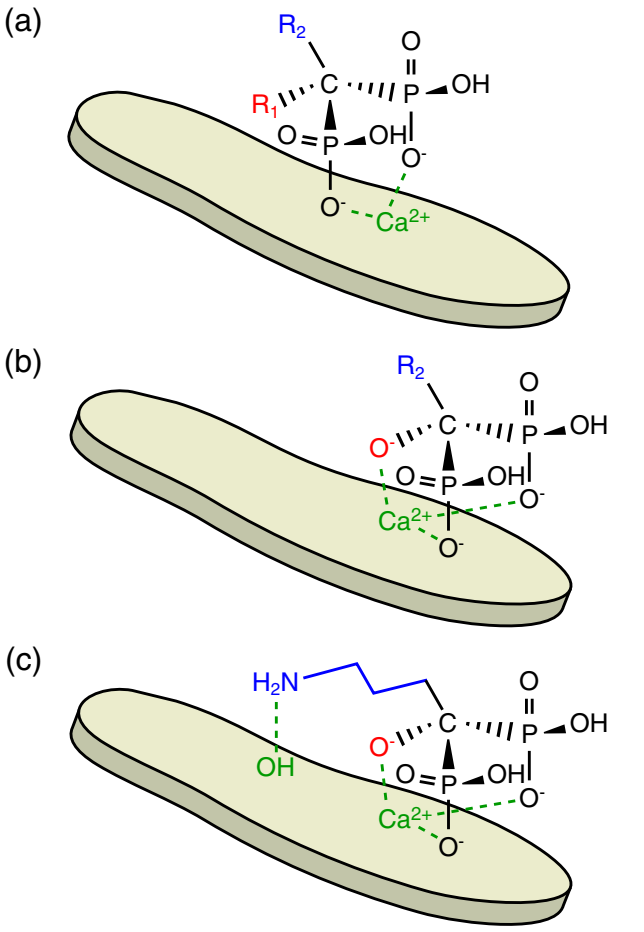

Fig. 3. Schematic representation of BP binding to a hydroxyapatite crystal surface, showing (a) bidentate binding involving the two phosphonates, (b) tridentate binding from the R_1 side group (OH), and (c) additional interactions from a nitrogen containing R_2 side group (*e.g.*, alendronate). These interactions have been investigated in detail using 3-D computational models [27,30].

3.3. Comparisons to other mineral-targeting ligands

Many other molecules besides BPs also exhibit bone-targeting characteristics. Many noncollagenous proteins that are found in bone exhibit binding affinity to hydroxyapatite [31] due to repeating amino acids such as glutamic or aspartic acid [32–34]. These amino acids exhibit a negative charge due to carboxylate ligands, which chelate calcium ions on the surface of hydroxyapatite. Peptides with glutamic acid and aspartic acid repeating units exhibited specific hydroxyapatite binding *in vitro* [34,35] and *in vivo* [35].

Direct comparisons between the binding affinity of BPs and glutamic or aspartic acid have varied in the literature. Peptides with eight repeating units of aspartic or glutamic acid exhibited faster and greater binding to hydroxyapatite compared with pamidronate or alendronate for up to 1 h *in vitro*, but a similarly high binding affinity for 2 to 24 h [36,37]. On the other hand, a peptide with six repeating units of aspartic acid did not exhibit greater binding to hydroxyapatite compared with tiludronate after 5 min incubation *in vitro* [35]. These studies suggest that the relative binding affinity of amino acids and BPs is governed by the number of peptide repeating units, the type of BP, and the incubation time.

Fundamental differences in the binding affinity of bone-targeting gold nanoparticles (NPs) have also been demonstrated. Gold nanoparticles

(Au NPs) surface functionalized with alendronate exhibited faster and greater binding to hydroxyapatite *in vitro* and damaged bone tissue *ex vivo* compared with glutamic acid or phosphonic acid [38,39]. The alendronate-functionalized Au NPs exhibited a six- or sixteen-fold greater binding affinity to hydroxyapatite when compared with glutamic or phosphonic acid-functionalized Au NPs, respectively, despite having fewer molecules adsorbed to the Au NP surface [38].

The use of amino acids as mineral targeting ligands has potential advantages and limitations compared with BPs. Unlike BPs, amino acids can be enzymatically degraded and cleared from the body after mineral binding [36], which minimizes the potential of cytotoxicity. However, the *in vivo* binding of aspartic acid to hydroxyapatite was lower compared with alendronate due to the high binding affinity of alendronate described above and possibly also due to rapid clearance of aspartic acid from circulation due to a highly negative charge [37]. Ligands which promote rapid clearance and excretion are expected to require a higher dose for effective mineral targeting compared with BPs, but this has not yet been confirmed by experiments. Although the remainder of this review will focus exclusively on the use of BPs, continued work to develop other mineral-targeting ligands is important for the future of mineral-targeting pharmaceuticals and imaging probes.

3.4. Common methods used to measure binding affinity

3.4.1. Langmuir adsorption isotherms

BP binding to mineral *in vitro* is most commonly modeled using Langmuir equilibrium adsorption isotherms as,

$$V = \frac{V_{max} \cdot K \cdot c}{1 + K \cdot c}$$

where V is the amount adsorbed (mol m^{-2}), V_{max} is the adsorption maximum (mol m^{-2}), c is the molar equilibrium solution concentration (mol L^{-1}), and K is the equilibrium affinity constant (L mol^{-1}) [27,40,41]. The adsorption maximum (V_{max}) and equilibrium affinity constant (K) are commonly calculated using linear regression after a double reciprocal transformation of the data [40]; however, nonlinear least squares regression provides a more powerful and direct method for determining these parameters from the data [38,40,42]. Langmuir adsorption isotherms enable quantitative comparison of the binding affinity between BPs and/or BP conjugates, where the binding affinity of a BP molecule may change after conjugation to a payload.

Studies which report only the percent of the initial BP concentration that binds to the mineral substrate for a given experiment only provide one data point within the overall binding equilibrium between BP and the mineral, and thus an incomplete picture. Moreover, the initial concentrations of the BP (or BP conjugate) and mineral substrate must be the same between experiments in order to compare results using percent binding. Therefore, initial *in vitro* experiments investigating the binding affinity of BPs or BP conjugates should measure the equilibrium binding constant (K) and adsorption maximum (V_{max}) from the Langmuir adsorption isotherm to enable comparison with other studies.

3.4.2. In vitro methods

The binding of BPs to hydroxyapatite mineral is commonly evaluated *in vitro* by incubating specified concentrations of BPs and hydroxyapatite crystals for a specified amount of time and then separating the unbound BP from the hydroxyapatite crystals with bound BP. The concentration of unbound BPs is measured using various methods described below, and the bound concentration is calculated from this data and the known initial concentration of BP. The most common methods for measuring the unbound BP involve labeling the BP or payload with radionuclides, nanoparticles, or aromatic residues. Common radionuclides include iodine-125 (^{125}I), technetium-99 (^{99m}Tc), and terbium-160 (^{160}Tb), which are detected using a gamma-counter and calibrated to known BP or payload concentrations [41,43–50]. BPs have been conjugated to gold nanoparticles allowing the initial and unbound concentration of gold to be measured using inductively coupled plasma optical emission spectroscopy (ICP-OES) [38,39,42] or ultraviolet (UV) absorbance [51]. Aromatic residues, which exhibit UV absorbance, were linked to peptides conjugated to BPs and the absorbance was correlated to the peptide concentration [36]. Note, that all the methods described above allow for the use of Langmuir models, but many of these studies only measured the percent binding of the BP conjugate for a single set of experimental conditions.

The crystal growth inhibition assay is another common *in vitro* method used to evaluate the binding affinity of BPs to hydroxyapatite mineral [11,52,53]. Briefly, hydroxyapatite crystals are formed in an environment with constant thermodynamic driving force (pH 7.4, 37 °C) [54] and a volume of titrant, which has a specific concentration of BP, is added to maintain this environment. The volume of titrant is measured as a function of time to calculate the crystal growth rate. This growth rate is related to the Langmuir equilibrium adsorption isotherm as,

$$\frac{R_o}{R_o - R_i} = 1 + \frac{1}{KC}$$

where R_o and R_i are growth rates (mol m^{-2} min^{-1}) in the absence and presence of BP, respectively, C is the molar concentration of BP in solution (mol L^{-1}), and K is the adsorption affinity constant (L mol^{-1}) [11].

Nuclear magnetic resonance spectroscopy (NMR) has also been used to measure the binding affinity of BPs to hydroxyapatite [55,56]. Solid-state NMR allowed for direct investigations of the molecular structure and binding energy of different BPs bound to hydroxyapatite [55], while liquid-state NMR was used to measure the concentration of unbound BPs, after incubating with hydroxyapatite, based on calibrations of the peak intensity [56]. Both solid-state and liquid-state NMR measurements allow for the use of Langmuir models.

The relative binding affinity of clinically available BPs has exhibited differences in rank order when using different *in vitro* measurement methods (Table 1). Although the differences are relatively small, it is important to recognize that different *in vitro* measurement methods can result in variations in measured binding affinities. Therefore, the reported binding affinity of a BP measured using one method should not be directly compared to that of a BP or BP conjugate measured a

Table 1
The relative binding affinity of common BPs measured *in vitro* by different methods.

Year	Study	Method	Substrate	Rank order[a]	Fold difference[b]
2006	Nancollas et al. [11]	Constant composition crystal growth	Hydroxyapatite	ZOL > ALN > IBN > RIS > ETO > CLO	1.6
2006	Leu et al. [57]	Radiolabeled	Human bone powder	ALN > ZOL ≈ PAM ≈ RIS > ETO > IBN > TLN > CLO	1.9
2008	Henneman et al. [52]	Constant composition crystal growth	Carbonated apatite	ZOL > ALN > RIS	1.17
2010	Lawson et al. [58]	Liquid chromatography	Hydroxyapatite	ZOL > RIS	1.4
2010	Jahnke et al. [56]	NMR	Hydroxyapatite	PAM > ALN > ZOL > RIS > IBN	2.1
			Human bone powder		1.95

[a] ALN = alendronate, CLO = clodronate, ETO = etidronate, IBN = ibandronate, PAM = pamidronate, RIS = risdronate, TLN = tiludronate, ZOL = zoledronate.
[b] Fold difference is based on the difference between the greatest and lowest binding affinities.

different method. Investigations of new BP molecules or conjugates require thorough characterization of the binding affinity.

The binding affinity of BPs to hydroxyapatite is also dependent on the *in vitro* environment, including the pH, ionic strength, and phosphate concentration [11]. Therefore, these factors should be noted in experimental methods. Additionally, the binding affinity measured *in vitro* should not be assumed to reflect the *in vivo* binding affinity, as the presence of serum proteins on the surface of mineral will reduce the overall binding *in vivo*. For example, media containing serum proteins dramatically reduced binding affinity of BP conjugates to hydroxyapatite *in vitro* [38,45], but may best mimic the *in vivo* interaction of BP and mineral surfaces [43].

3.4.3. In vivo methods

The delivery and binding of BPs *in vivo* are also commonly monitored using radiolabeled-BP conjugates, such as ^{125}I- or ^{99m}Tc-labeled BPs or BP complexes. Radiolabeled BP conjugates are delivered intravenously and animals are euthanized after a specified time to measure the concentration of radionuclide in explanted tissues [43,44,46,49,59–62]. The biodistribution of BPs has been commonly measured in bones, such as femora and tibiae, and organs, such as the kidneys, liver, spleen, heart, intestines, and brain. The concentration of BPs in the blood is measured as the bone-to-blood ratio to examine the clearance of BPs from the blood and the binding of BPs to bone. Radionuclide-labeled BPs can also be used to monitor BP binding and biodistribution longitudinally *in vivo*, avoiding the need to euthanize animals at each study time point [47]. However, as will be discussed below, the short-half life of radionuclides prevents tracking BPs *in vivo* over time periods exceeding 24 h. Therefore, BPs were recently conjugated to fluorophores in order to monitor the biodistribution, binding, and retention of BPs *in vivo* for up to 7 days after administration [63].

The ability to track BPs *in vivo* provides investigators with a powerful tool to investigate the targeted delivery and biodistribution of BP conjugates. The uptake and distribution of BPs in the skeleton is influenced by the delivery route and sites of active bone remodeling. Oral administration results in only ~0.7% of the total dose reaching the skeleton, while ~65% of the total dose reaches the skeleton after intravenous administration [64,65]. BP uptake is greater in trabecular bone compared with cortical bone due to greater blood flow, surface area, and bone turnover in trabecular bone [64]. BPs also accumulate in active sites of bone resorption more than bone formation due to a larger area of exposed hydroxyapatite crystals available for BP binding. Importantly, the uptake and biodistribution of BPs may be altered by the addition of a payload. Therefore, evaluations of BP conjugates require the ability to track BP conjugates *in vivo* over extended time periods after delivery.

4. Applications of bisphosphonates as a targeting ligand

4.1. Therapeutic drug delivery

4.1.1. Metabolic bone disease

Osteoporosis and other metabolic bone diseases are commonly treated with BPs [16,66] due to the high binding affinity of BPs to bone and their ability to inhibit bone resorption by promoting osteoclast apoptosis [18]. A number of recent reviews have thoroughly summarized the current state of knowledge of BPs used clinically (Fig. 2) as therapeutics for metabolic bone diseases [67–69]. Therefore, this information will not be covered here, although it is important to note that there has been mounting concern over limitations and potential negative side effects associated with long-term use of BPs [17], which has led to intense investigation of other potential drugs and targets to treat metabolic bone diseases. We will instead focus on BP conjugates investigated as therapeutics for metabolic bone diseases.

Molecular complexes have been formed by conjugating BPs to either catabolic (inhibitors of bone resorption) or anabolic (inducers of bone formation) drugs (Table 2). BPs were conjugated to many of these agents to enable targeted delivery of drugs that would otherwise have no affinity to bone. Thus, the functional role of the BP molecule in these complexes is exclusively for targeted delivery and not pharmacological activity, although clinical translation will require investigation of the latter given the known activity of BPs.

Estrogen replacement therapy has been considered an option to treat postmenopausal osteoporosis as estrogen depletion is known to decrease bone mass [70]. However, systemic delivery of estrogen has limited efficacy as estrogen receptors are present in many tissues besides bone tissue and increased levels of estrogen in postmenopausal women have been associated with an increased risk of certain cancers, such as breast or uterine cancer [70]. Therefore, various schemes have been investigated to conjugate BP to 17β-estradiol as means to increase the dose of estrogen delivered to bone tissue, while decreasing estrogen accumulation in other soft tissues [71–76]. The *in vivo* efficacy of these complexes has varied from no added benefit of the bone-targeting ligand [71] to a selective increase in bone mineral density compared with weight change of the uterus, indicating that the BP ligand enabled targeted delivery of 17β-estradiol [72,73]. The reason for the difference in the efficacy between these studies may be due to a difference in the dose of 17β-estradiol delivered, with the higher dose stimulating an increase in bone mass and demonstrating benefit of the BP targeting ligand [72,73].

BPs have also been conjugated to other anabolic agents such as prostaglandin E_2 [77], agonists against the EP4 receptor for prostaglandin E_2 [78], and parathyroid hormone (PTH) [79]. Prostaglandin E_2 is an enzymatically-derived metabolite of polyunsaturated fatty acids, which can stimulate bone formation leading to increased bone mass

Table 2
Pharmaceutical drugs conjugated to BPs to treat metabolic bone diseases.

Drug[a]	Summary of results	Reference(s)
17β-estradiol	Bone loss was inhibited in rat models of osteoporosis.	Bauss et al. [71] Fujisaki et al. [72,73] Page et al. [74,75] Morioko et al. [75]
PGE_2	Bone formation was stimulated *in vivo* at a 30-fold lower dose than free PGE_2. Cortical bone osteopenia was not able to be recovered in rats.	Gil et al. [77]
Agonist against EP4 receptor	~6–9% of the initial dose was taken up by long bones in rats and the drug was released with a half-life up to 2 weeks. The therapeutic efficacy has not been examined.	Arns et al. [78]
PTH	*In vitro* binding to hydroxyapatite was greater than free PTH. Bioactivity was greater than free PTH during *in vitro* cell culture.	Yewle et al. [79]
Calcitonin	A high binding affinity was measured both *in vitro* and *in vivo*. Therapeutic efficacy was greater than free calcitonin in an osteoporotic rat model.	Bhandari et al. [81,84] Yang et al. [47]
OPG	A two- and four-fold greater uptake was enabled in normal and osteoarthritic bone, respectively, compared with free OPG.	Doschak et al. [48]

[a] EP4 = prostaglandin E receptor 4, OPG = osteoprotegerin, PGE_2 = prostaglandin E_2, PTH = parathyroid hormone.

[80], but undesired side effects after systemic delivery of prostaglandin E_2 has limited use as a therapeutic. Therefore, alendronate was conjugated to prostaglandin E_2 for targeted delivery to mineral which was verified *in vitro* and *in vivo* [77]. Unfortunately, neither the alendronate-conjugated prostaglandin E_2 nor free drug were able to overcome the bone mass loss in a rat model of osteoporosis, possibly due to instability of the prostaglandin E_2 molecule [77]. Therefore, alendronate ligands were conjugated to an agonist against the EP4 receptor for prostaglandin E_2 in an attempt to improve *in vitro* stability and therapeutic efficacy compared with BP-conjugated prostaglandin E_2 complexes [78]. This complex enabled targeted delivery *in vivo*, but the biological efficacy has not yet been evaluated. PTH is another promising anabolic agent to treat osteoporosis that is limited by a broad biodistribution and inefficient targeting after systemic delivery. PTH was conjugated with BP ligands *via* a hydrazine linkage, resulting in targeted delivery to bone *in vitro* while retaining the biological activity of PTH [79].

Antiresorptive agents, including calcitonin [47,81] and osteoprotegerin [48], have been investigated as alternatives to BPs for the treatment of osteoporosis. Calcitonin is used in the treatment of Paget's disease, bone metastases, and osteoporosis [82], which inhibits osteoclast-mediated bone resorption [83]. However, free calcitonin has a very short half-life and is rapidly cleared from the body, reducing the dose that reaches the bone. Furthermore, calcitonin receptor is expressed by non-skeletal cell types in addition to osteoclasts, which also reduces the dose delivered to the bone. Therefore, calcitonin was conjugated with BP for targeted delivery to bone [47,81]. BP-conjugated calcitonin exhibited high binding affinity to hydroxyapatite mineral *in vitro* and bone *in vivo* compared with free calcitonin [47,81,84], and the biological cellular activity of calcitonin was maintained after BP conjugation [81,84]. BP-conjugated calcitonin also preserved the bone volume and bone mineral density more than non-targeted calcitonin in a rat model of osteoporosis [84]. Osteoprotegerin is a factor that disrupts the RANK–RANKL signaling pathway, leading to decreased osteoclastogenesis [48]. BP-conjugated osteoprotegerin exhibited greater hydroxyapatite binding *in vitro* and bone binding *in vivo* compared with free osteoprotegerin [48]. However, the biological activity and therapeutic efficacy of BP-conjugated osteoprotegerin has not yet been evaluated.

The concept of conjugating BPs to proteins that promote bone formation and healing was introduced by Uludag and coworkers in 2000 [45] and has continued into the present with a significant body of work reviewed elsewhere [59,85,86]. Protein-based therapeutics are promising options to treat bone diseases by directly modulating cellular signaling mechanisms [85]. However, most proteins do not exhibit specific binding to hydroxyapatite but have ubiquitous targets throughout the body. Therefore, BP molecules could be conjugated to proteins to improve bone-targeting, reduce the required dose, and reduce extraosseous accumulation of the proteins. BPs have been conjugated to many model proteins, such as bovine serum albumin, lysozyme, and IgG, and exhibited increased bone uptake compared with free protein *in vivo* [45,61]. Therefore, these studies suggest that BPs can be used as a targeting ligand to deliver proteins to bone tissue.

4.1.2. Bone cancer and metastases

The skeleton is a common site for cancer metastasis [87,88]. Tumors in the skeleton alter the normal homeostasis of bone by disrupting the bone remodeling cycle which leads to bone pain, fractures, and hypocalcemia [89]. Treatment options are typically limited to reducing bone pain *via* palliative radiation therapy, analgesics, or BPs [89]. Radiotherapy and chemotherapy agents can be used to treat the tumor, but are not always successful depending on the tumor type [90]. BPs can be used to treat and prevent skeletal morbidity or hypercalcemia associated with metastases [89,90]. Recent preclinical studies have provided evidence that BPs may also have an antitumor effect by inducing cancer cell apoptosis and inhibiting cell invasion [91], suggesting that BPs may be used to treat the tumor in addition to the surrounding bone.

The need for improved therapeutics is particularly great in bone cancers due to the problems associated with surgical resection of skeletal lesions and the development of chemoresistant tumors. As with many cancer types, targeted therapies are being investigated as a means to improve therapeutic outcomes by enabling the delivery of a high concentration of an antitumor agent to the tumor site and reducing adverse side effects associated with systemic delivery of non-targeted drugs [92]. Therefore, the high binding affinity of BPs for bone is being investigated as a means to enable targeted delivery of antitumor agents to metastases (Table 3) to promote the accumulation of BPs in areas of high bone turnover resulting in greater retention of BP conjugates in cancerous lesions compared with healthy bone.

One of the first studies demonstrated that cisplatin conjugated with phosphonates exhibited greater antitumor activity compared with cisplatin alone in an osteosarcoma model in rats [93], but did not determine whether the enhanced activity was due to targeted delivery or the combined antitumor effects of cisplatin and BP. BP–cisplatin conjugates were more recently shown to enhance anticancer effects compared with cisplatin alone using an *in vitro* cell culture model where delivery does not play a role [94]. Therefore, future studies need to measure the accumulation of BP–cisplatin conjugates in bone metastases *in vivo* and compare the therapeutic efficacy of BP–cisplatin *versus* cisplatin alone, BP alone, and co-delivery of cisplatin and BP alone. Other BP-conjugated chemotherapy agents that have been investigated include BP conjugated to taxanes [95–97], platinum complexes [98], camptothecin [99], gemcitabine [49,100–102], doxorubicin [103,104], methotrexate [105], proteasome inhibitors [106,107], arabinocytidine [108], and an anti-angiogenic agent, TNP-470, which is a synthetic analog of fumagillin [109]. Overall, BP conjugation has been repeatedly shown to improve targeted delivery of these agents to bone metastases.

Table 3
Antitumor agents conjugated to BP for the treatment of bone cancers.

Drug	Summary of results	Reference(s)
Cisplatin	Anti-tumor activity was greater than the non-targeted drug *in vivo*.	Klenner et al. [93]
Taxanes	A high binding affinity was exhibited to hydroxyapatite *in vitro* and bone tumors *in vivo*.	Miller et al. [95]
	Anti-tumor activity was greater than the non-targeted drug and free BPs, *in vitro* and *in vivo*.	Miller et al. [96] Chaudhari et al. [97]
Camptothecin	A high binding affinity to hydroxyapatite was exhibited *in vitro*.	Erez et al. [98]
Gemcitabine	A high binding affinity was exhibited to hydroxyapatite *in vitro* and bone *in vivo*.	El Mabhouh et al. [99], 2006
	Anti-tumor activity was greater than the free drug and control groups *in vivo*.	[49] [104] [103]
Doxorubicin	A high binding affinity to hydroxyapatite was exhibited *in vitro*.	Hochdörffer et al. [104]
Methotrexate	A high binding affinity to bone was exhibited *in vivo*.	Hosain et al. [105]
Proteasome inhibitors	Binding to hydroxyapatite was greater than the non-targeted drug *in vitro* and *in vivo*.	Agyin et al. [106]
	Anti-tumor activity was greater than the non-targeted drug, *in vitro* and *in vivo*, leading to increased overall survival of mice.	Swami et al. [107]
Arabinocytidine	The incidence of bone metastases and overall tumor burden was decreased in mice compared with no drug or zoledronate at the same dose.	Reinholz et al. [108]
TNP-470	Anti-tumor activity was greater and cytotoxicity lower than the non-targeted drug or alendronate *in vivo*.	Segal et al. [109]

In some cases, targeted delivery reduced systemic toxicity compared with the free drug and/or free BP [96,104,109].

4.1.3. Other bone diseases

Inflammatory bone diseases include osteomyelitis, which is an infection in the bone that causes an inflammatory response and bone necrosis [110], and rheumatoid arthritis, which is an autoimmune disorder that can eventually lead to bone erosion [111]. Both of these diseases must be treated with large doses of pharmaceuticals in order to deliver a sufficient amount to the bone [112]. Targeted delivery of antibiotics or anti-inflammatory agents could help to reduce the overall dose.

Antibacterial agents conjugated with BPs exhibited 13-fold greater binding to bone powder compared with the free agents and were able to inhibit bacterial growth in an *in vitro* model of osteomyelitis even after the BP-antibacterial conjugate was first bound to the bone *ex vivo* [113]. More recently, prodrugs have been developed to release the antibacterial agent from the BP conjugate in order to improve the biological activity of the drug [112,114]. These BP-antibacterial agent prodrugs exhibited high binding affinity and activity both *in vitro* and *in vivo* [114].

Diclofenac is an anti-inflammatory drug used to treat rheumatoid arthritis, which can lead to negative gastrointestinal side effects [115]. BP–diclofenac conjugates have been developed as a bone-targeted drug to treat inflammatory bone diseases [116,117]. BP–diclofenac conjugates exhibited greater bone accumulation *in vivo* compared with free diclofenac [116] and improved therapeutic efficacy, as measured by a reduction in the mean effective dose that was necessary to reduce swelling in a rat model of arthritis and a reduction in side effects compared with the free drug [116]. However, it is important to note that the accumulation of BP–diclofenac in the liver was dose-dependent; a 10-fold increase in administered dose resulted in decreased bone accumulation but increased liver accumulation [116,117]. Therefore, dose escalation studies will be important to determine the most appropriate dose for therapeutic efficacy.

Legg–Calvé–Perthes disease results in osteonecrosis of the hip joint in children due to a temporary block in the blood supply [118]. BP-functionalized gold nanoparticles were proposed as a drug delivery system to treat osteonecrosis [119]. Osteoclastogenesis and osteoclast function was decreased *in vitro* after incubation with BP-functionalized gold nanoparticles, but not citrate-coated gold nanoparticles [119]. Interestingly, the ability of BP-functionalized gold nanoparticles to induce osteoclast apoptosis *in vitro* demonstrated that the cellular activity of BP was not hindered after conjugation to a payload. However, the delivery of BP-functionalized gold nanoparticles to areas of osteonecrosis *in vivo* may be challenging due to a lack of blood supply and must be evaluated.

4.1.4. Engineered drug delivery platforms

Synthetic polymers and nanoparticles have been conjugated to BPs and investigated as drug delivery platforms for a variety of applications. Synthetic polymers such as poly(ethylene glycol) (PEG) [37,51,120], poly(ethylenimine) [121], poly(L-lysine) [121], *N*-(2-hydroxypropyl) methacrylamide (HPMA) [37,58], and poly(γ-benzyl-L-glutamate) (PBLG) [122] have been conjugated to BP as versatile bone-targeting drug carriers and have universally exhibited high binding affinity to hydroxyapatite. Water-soluble polymers [123] are attractive drug carriers due to biocompatibility, biodegradation *in vivo*, and an ability to increase the water solubility of many hydrophobic drugs. Additionally, polymers can be used to increase the size of small molecule drugs and thereby limit the biodistribution [62], which might increase the dose that can be delivered to challenging targets like bone.

BP-functionalized nanoparticles have been developed as carriers to deliver drugs to bone. The goal of using nanoparticles for drug delivery is to enable (1) specific drug targeting and delivery, (2) reduced off-target side effects, and (3) increased therapeutic efficacy through higher delivered doses [124]. Nanoparticles can also enable the drug to be encapsulated, instead of conjugated to the nanoparticle surface, which may be advantageous if chemical conjugation affects the drug activity [60]. The majority of BP-functionalized nanoparticle drug delivery systems have consisted of liposomes [125–128] or polymeric nanoparticles [107,129–132], as these are readily loaded with a variety of different drugs and surface functionalized with BP molecules. Calcium phosphonate nanoparticles were also conjugated with BP and proposed as a highly biocompatible bone-targeted drug delivery system [133]. BP-functionalized nanoparticles have almost universally exhibited high binding affinity to hydroxyapatite *in vitro* regardless of the payload (*e.g.*, liposome *versus* polymer) [107,125–129,132,133], although there have been no direct comparisons between different systems.

4.2. Imaging

Bone-targeting nuclear imaging agents were among the first applications of BPs with the introduction of ^{99m}Tc and BP conjugates in the 1970s [134]. Bone scintigraphy has become a common nuclear imaging technique with more than 3 million bone scans performed in the United States in 2005 [135]. ^{99m}Tc–BP conjugates are delivered intravascularly and target exposed hydroxyapatite mineral such that uptake is imaged to detect areas of high bone turnover, such as Paget's disease lesions and bone cancers or metastases.

The chemical structure of clinically available ^{99m}Tc–BP conjugates, such as ^{99m}Tc-methylene diphosphonate (^{99m}Tc-MDP) and ^{99m}Tc-hydroxymethylene disphosphonate (^{99m}Tc-HMDP), are not ideal for the intended application of targeting and labeling areas of high bone turnover for non-invasive imaging [136]. A lack of chemical stability *in vivo* reduces specificity due to lower bone uptake and higher soft tissue uptake of ^{99m}Tc [136]. Furthermore, slow blood clearance or bone uptake requires long time intervals between administration and imaging (~3–4 h) [136]. The chemical structure of ^{99m}Tc–BP conjugates are not well-defined, but are thought to be mixtures of monomers and polymer species which have different properties leading to low overall efficacy and consequently requiring the administration of high doses [136]. Furthermore, the BP acts as both the radionuclide chelator and bone-targeting ligand [137] (Fig. 4a). This dual function of the BP molecule lowers the overall binding affinity of ^{99m}Tc–BP conjugates due to only one of the phosphonate groups being free for binding to hydroxyapatite surfaces [138].

The limitations of ^{99m}Tc–BP conjugates have motivated research aimed at improving radionuclide–BP conjugates for bone scintigraphy, as well as research for new targeted imaging agents for other imaging modalities, such as near-infrared (NIR) fluorescence imaging, positron emission tomography (PET), magnetic resonance imaging (MRI), and X-ray imaging with computed tomography (CT). New imaging agents are developed for the goal of improved clinical diagnostic imaging of bone metabolism, bone metastases, or pathological calcifications. Additionally, new imaging agents that are designed to track BP *in vivo*

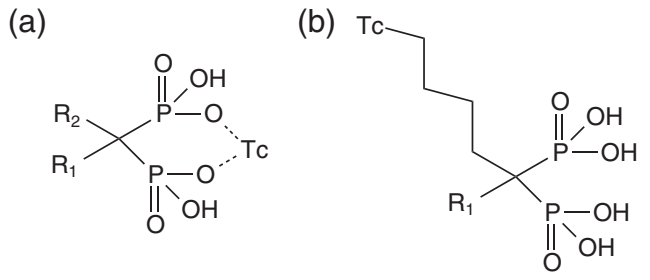

Fig. 4. Molecular structure of ^{99m}Tc-BP conjugates. (a) In the ^{99m}Tc-BP conjugates currently used clinically, the BP acts as both the radionuclide chelator and bone-targeting group, which potentially limits the bone targeting capacity of these agents *in vivo*. (b) Bifunctional chelating ligands are being investigated as linkers between the BP and radionuclide, freeing the phosphonate groups to function exclusively for bone-targeting.

can facilitate improved understanding of BP binding, biodistribution, and pharmacokinetics in preclinical drug development.

4.2.1. Novel bone scintigraphy agents

A number of studies have investigated the use of bifunctional chelator ligands to separate the BP from the radionuclide (Fig. 4b), allowing the BP to function exclusively for bone-targeting [23,138–144]. The availability of both phosphonate groups for bone-targeting results in increased binding affinity, increased kinetics for bone uptake, decreased soft tissue uptake, and reduced time required between administration and imaging [138]. Examples of bifunctional chelator ligands include 6-hydrazinopyridine-3-carboxylic acid (HYNIC) [138,142], pyrazolyl-containing backbones [139,140], and diethylene triamine pentaacetic acid (DTPA) [144], among others [23,141,143]. ^{99m}Tc–bifunctional-BP complexes exhibited increased *in vitro* binding affinity and faster binding kinetics to hydroxyapatite crystals compared with ^{99m}Tc-MDP [23,138]. A few ^{99m}Tc–bifunctional-BP complexes have enabled higher bone uptake *in vivo* compared with ^{99m}Tc-MDP [138,142,143], although others have exhibited similar bone uptake at the time points investigated [23,140]. Therefore, the greatest benefit of the bifunctional ligands has thus far been a greater bone-to-blood ratio of the ^{99m}Tc–bifunctional-BP complexes [138,140,142,143], which should reduce the time delay between contrast agent administration and imaging.

4.2.2. Targeted fluorescence imaging

Fluorescently-labeled BPs have been investigated for monitoring bone metabolism and for tracking the biodistribution of BPs *in vivo*. The first NIR fluorescent BP conjugate was developed by Frangioni and coworkers in 2001 by conjugating pamidronate to the NIR fluorophore, IRDye78 [25]. The conjugate enabled *in vivo* fluorescence imaging of osteoblast activity in mice with greater sensitivity and spatial resolution compared with bone scintigraphy using ^{99m}Tc-MDP, suggesting that NIR-BP conjugates could be used for non-invasive imaging of bone activity. This conjugate also enabled *in vivo* fluorescence imaging of vascular calcifications [145] and breast microcalcifications [26,146], including dual-mode NIR/SPECT imaging of breast microcalcifications when combined with ^{99m}Tc-MDP [28].

NIR-BP imaging probes using pamidronate recently became commercially available (OsteoSense™, Perkin Elmer) and have been used in a wide range of preclinical animal models investigating, for example, noninvasive, longitudinal imaging of bone metabolism [147–150] (Fig. 5a), site-specific BP deposition and retention [148], bone regeneration in novel tissue engineering applications [151], and the formation of pathological calcifications such as kidney stones [152], vascular calcifications [153] (Fig. 6a), and breast microcalcifications [154]. Additional novel NIR probes conjugated to BPs other than pamidronate have also been developed, including alendronate [155] and risedronate [156]. NIR imaging was therefore also used to compare differences in the binding affinity and biodistribution of different BPs *in vivo* [63] (Fig. 5b).

Bone-targeting fluorescent imaging probes have become powerful tools in preclinical animal models to monitor bone metabolism or track BP *in vivo* as longitudinal imaging can be conducted over weeks. This is a direct advantage over ^{99m}Tc-BP agents and nuclear imaging as ^{99m}Tc has a biological half-life of only one day which prevents studying the retention of BPs *in vivo* [148]. Additionally, the high sensitivity of optical imaging techniques enables detection of very small pathological calcifications, which could provide a means to study the initial formation of these mineral deposits *in vivo*. However, fluorescence imaging of bones in humans is limited by the overall depth penetration. Frangioni and coworkers calculated an exponential decay constant of $k = -0.43\ \mathrm{mm}^{-1}$ from their experiments using IRDye78 *in vivo*, demonstrating that the NIR signal intensity decreased by 50% at 2.5 mm from the skin surface [25]. Therefore, despite their utility in preclinical studies, bone-targeted fluorescent probes are not likely to replace the current bone scintigraphy agents, such as ^{99m}Tc-MDP, for clinical imaging in humans.

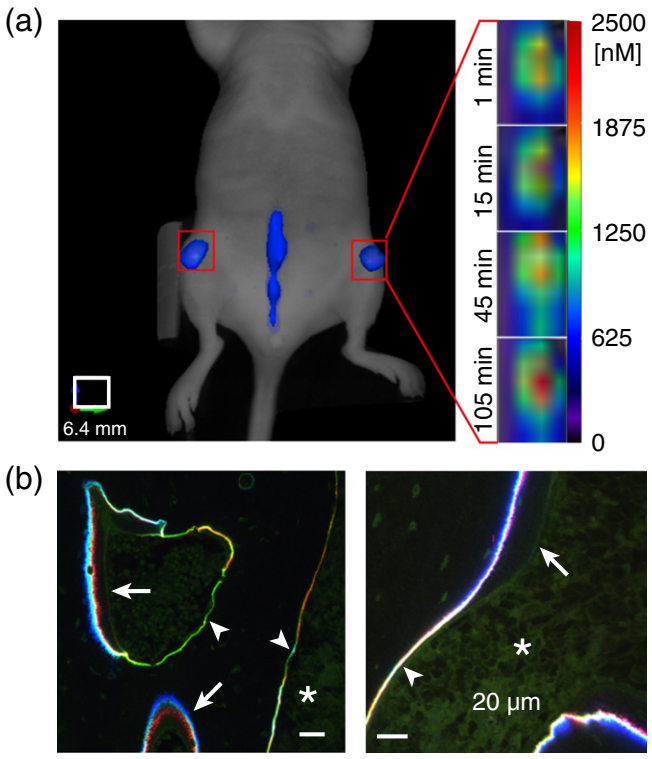

Fig. 5. Examples of *in vivo* bone-targeted fluorescence imaging using BP conjugates. (a) A fluorescently-tagged BP was delivered to mice *in vivo* and the accumulation of BP at the tibia was monitored using fluorescent molecular tomography. Reprinted with permission from Tower et al. 2014 [149]. (b) Risedronate and two lower binding affinity analogs were conjugated to fluorescent molecules and co-administered to growing rats *in vivo* to investigate differences in the biodistribution, binding, and retention of BPs with different affinity within bone. In sites with active formation (arrows), the lower affinity BP (blue) was found buried underneath newly formed bone, while the higher affinity BP (red) was closer to the newly formed surface. In quiescent sites (arrowheads), there was no difference in penetration depth. Reprinted with permission from Roelofs et al. 2012 [63].

4.2.3. Targeted PET, MRI, X-ray imaging

Although clinical use of targeted BP imaging agents has been dominated by bone scintigraphy, there have been recent efforts to develop BP-functionalized contrast agents for other imaging modalities, including positron emission tomography (PET), magnetic resonance imaging (MRI), and X-ray imaging with computed tomography (CT). Bone or mineral targeted imaging agents for PET, MRI, and CT could provide a translational pathway for improved clinical diagnostic imaging of skeletal abnormalities, such as tumors or pathological calcifications. Na^{18}F-fluoride PET is already used clinically for imaging bone metastases and is considered superior to ^{99m}Tc-MDP scintigraphy due to a demonstrated increase in sensitivity and specificity [157]. Additionally, PET imaging can be conducted 30–90 min after contrast agent administration compared with 3–6 h for bone scintigraphy [157]. However, Medicare and Medicaid will not currently reimburse providers for PET imaging of benign diseases [135], inhibiting widespread use. MRI enables high spatial resolution and detection sensitivity without radiation exposure to the patient [158]. Although MRI produces strong soft tissue contrast, contrast agents are needed to image mineralized tissues or deposits [159]. CT provides anatomic imaging with high spatial and temporal resolution [158], especially for bone. CT also offers relatively wide availability and lower cost compared with MRI and PET, and lower radiation exposure than SPECT or PET, which utilize radioisotopes and require combined CT for anatomic imaging. However, CT has a relatively low sensitivity compared to SPECT, PET, or MRI, and low soft tissue contrast compared with MRI [160].

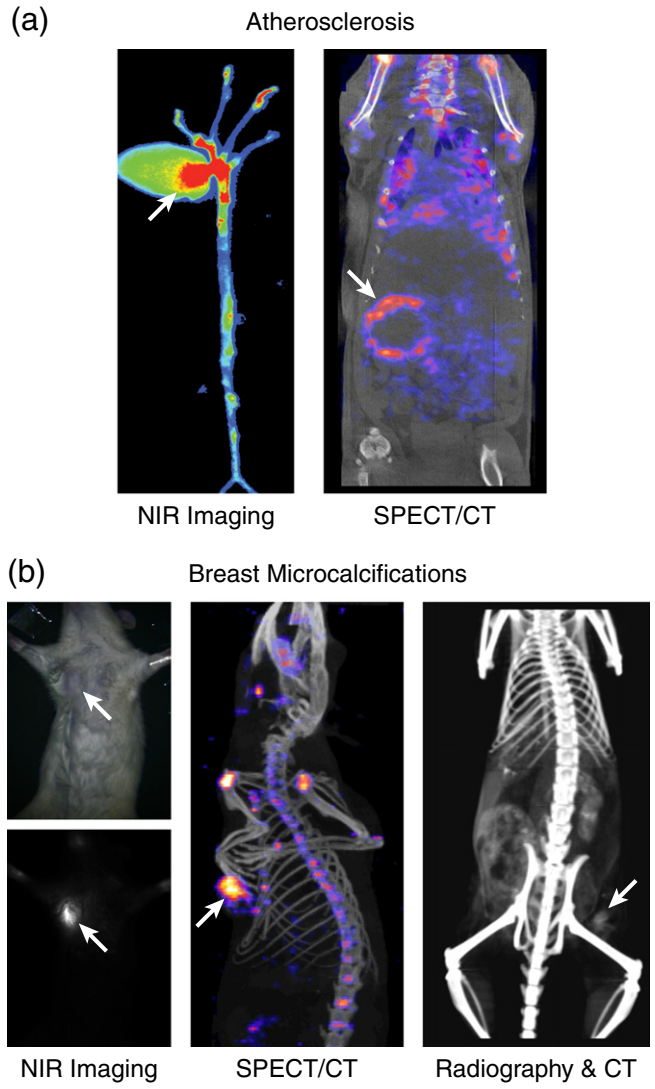

Fig. 6. BP-conjugated imaging probes have been developed for targeting bone and pathological calcifications in a wide array of imaging modalities, including nuclear (SPECT, PET), optical (NIR fluorescence), MRI, and X-ray (CT) imaging. (a) Atherosclerotic vascular calcifications have been targeted and imaged in rodents *in vivo* with probes comprising BPs conjugated to NIR [153] or SPECT [174] contrast agents. (b) Breast microcalcifications associated with cancer were also targeted and imaged *in vivo* using probes comprising BPs conjugated to NIR, SPECT, and X-ray/CT contrast agents. The NIR and SPECT images were adapted with permission from Bhushan et al. 2008, J Am Chem Soc, 130:17648–17649 [28]. Copyright 2008 American Chemical Society. X-ray image adapted with permission from Cole et al. 2014, ACS Nano, 8:7486–7496 [169]. Copyright 2014 American Chemical Society.

PET and MRI agents rely on the conjugation of BP molecules to a chelator, such as 1,4,7,10-tetraazacyclododecane-1,4,7,10-tetraacetic acid (DOTA) or 1,4,7-triazacyclononane-*N,N′,N″*-triacetic acid (NOTA), which complex with positron-emitting radionuclides for PET imaging or lanthanide metals for MRI imaging [136]. A BP-DOTA conjugate, (4-{[(bisphosphonomethyl)carbamoyl]methyl}-7,10-bis(carboxymethyl)-1,4,7,10-tetraazacyclododec-1-yl)acetic acid (BPAMD), was first introduced in 2005 as a bone targeting chelator for gadolinium (Gd) to create Gd(III)-BPAMD complexes for T1 MRI imaging [161]. Gd(III)-BPAMD binding to hydroxyapatite *in vitro* led to a significant increase in MRI relativity demonstrating the potential of this contrast agent to enable MRI imaging of bone mineral [161]. Novel PET agents have been synthesized by labeling BPAMD with positron-emitting gallium-68 ([^{68}Ga]BPAMD) [162–164]. The first human clinical study demonstrated greater uptake and improved detection of bone metastases with [^{68}Ga]BPAMD compared with the current clinically available PET agent, ^{18}F-fluoride [162]. In general, BP-DOTA conjugates have exhibited high binding affinity *in vitro* [50,161,163,165–167] and *in vivo* [162–167]. BP-DOTA conjugates also exhibited greater binding affinity than ^{99m}Tc-MDP [164,165], indicating their utility for bone-specific imaging using PET or MRI, comparable to bone scintigraphy.

Recently, other BP–DOTA conjugates have been synthesized for PET and MRI to improve the *in vivo* binding affinity and blood clearance by altering the structure or increasing the length of the spacer between the BP and DOTA or NOTA [41,165,167]. The replacement of an amine group at the link between DOTA and BP with a negatively charged phosphonic acid group resulted in greater binding affinity *in vitro* [41] and *in vivo* [167] compared with BPAMD, and similar bone uptake compared to ^{99m}Tc-MDP and ^{18}F-fluoride [164]. [^{68}Ga]NOTA–BP agents exhibited high binding affinity to hydroxyapatite *in vitro* and bone *in vivo*, as well as a greater bone-to-blood ratio compared with ^{99m}Tc-MDP and ^{18}F-fluoride [165]. Therefore, these new BP–DOTA conjugates with greater separation between DOTA and BP are promising for PET and MRI imaging of bone or mineral pathologies [136]. However, the higher cost of PET or MRI compared with bone scintigraphy may inhibit widespread clinical use of these technologies for bone imaging.

X-ray contrast agents based on BP-functionalized gold nanoparticles (BP-Au NPs) were investigated as potential imaging agents for microdamage in bone tissue [38,39,42] and pathological calcifications, specifically breast microcalcifications [168,169], based on the high binding affinity of BP-Au NPs to hydroxyapatite [38]. Au NPs were surface functionalized with alendronate through adsorption of the amine side group to the Au NP surface opposite the two phosphonate groups for binding to hydroxyapatite [38]. BP-Au NPs targeted microcalcifications due to specific binding to hydroxyapatite and enabled improved sensitivity and specificity *via* contrast-enhanced detection of model breast microcalcifications within the surrounding mammary tissue [168,169], including radiographically dense mammary tissues [170].

The major challenge for the use of targeted contrast agents to image bone or pathological mineral deposits with CT is the need to deliver a sufficient mass concentration for contrast enhancement [171]. For example, the theoretical minimum detectable mass concentration of gold in bone is ~0.34 wt% or ~3.4 mg Au/g bone tissue [171,172]. Thus, CT has a relatively low sensitivity and requires higher concentrations of contrast agents compared with MRI, which can detect millimolar concentrations, or nuclear imaging (SPECT, PET), which can detect micromolar concentrations [173].

In summary, BP-conjugated imaging agents have been developed for nuclear (SPECT, PET), optical (NIR), MRI, and X-ray (CT) imaging. Depending on the intended target, BPs can be conjugated to an imaging probe for any of the different modalities (Fig. 6). For example, atherosclerotic vascular calcifications have been targeted and imaged *in vivo* using BP-conjugated NIR [153] or SPECT [174] contrast agents (Fig. 6a), while breast microcalcifications associated with cancer were also targeted and imaged *in vivo* using BP-conjugated NIR [29], SPECT [29], and X-ray/CT [169,170] contrast agent (Fig. 6b). A logical next step will be to combine or design BP-conjugated imaging probes for dual- or tri-modal imaging. For example, Bhushan et al. developed a novel NIR/SPECT probe for imaging breast microcalcifications [29], which could be used to target and image bone metastases as well as to asses the utility of NIR imaging *in vivo.*

4.3. Radiotherapy

Targeted radiotherapy to the skeleton is currently used clinically to treat pain caused by bone metastases [136]. In particular, internal radiotherapy uses close-range α-, β-, and γ-emitting radionuclides, which are targeted to the skeleton and selectively taken up by bone metastases to deliver a high local dose of radiation. Samarium-153-ethylene diamine tetramethylene phosphonate (^{153}Sm-EDTMP) has proven clinically effective in reducing the pain associated with bone metastases [175]. The phosphonic acid group (EDTMP) is complexed to Sm and facilitates

binding of the radionuclide to bone. However, this complex is very unstable *in vivo* and thus requires co-administration of free EDTMP [176]. Rhenium-188 (^{188}Re) is a radionuclide, similar in chemistry to ^{99m}Tc, which has been complexed with HEDP (^{188}Re-HEDP) as a targeted radionuclide [177], similar to ^{99m}Tc-HEDP agents. Clinical trials have indicated that ^{188}Re-HEDP may be effective as a β-emitting radiotherapy agent for bone metastases [177]. However, similar to the disadvantages of ^{99m}Tc-HEDP discussed above, ^{188}Re-HEDP degrades quickly *in vivo* inhibiting retention of the radionuclide at the lesion [136].

New BP-radionuclide conjugates are being investigated to improve chemical stability and binding affinity for delivery of a high local dose to bone metastases. Bifunctional ligands are being investigated to separate the BP molecule from the radionuclide chelating groups, using parallel strategies discussed above for ^{99m}Tc-BP conjugates. Isolating the BP molecule from the radionuclide enables both phosphonate groups to bind to mineral surfaces. This strategy resulted in increased *in vivo* binding and accumulation in areas of high bone turnover compared with ^{188}Re-HEDP agents in mice [176,178,179]. Many other radionuclides, including ^{211}At [180,181], ^{160}Tb [50], and ^{125}I or ^{131}I [180,182] have been conjugated with BPs and investigated in preliminary studies for targeted radiotherapy using different emitters.

5. Design considerations for future investigations

The use of BPs as a targeting ligand for the delivery of therapeutic drugs or imaging probes requires the design of novel molecular conjugates (Fig. 1). The functional requirements of these conjugates are to target and bind to mineral with high affinity, while not altering the function of the therapeutic agent or imaging probe that is being delivered. These functional requirements can be met by designing the molecular structure of the conjugates, but systematic study of structure-function relationships has been lacking. Therefore, we have identified several key aspects of molecular structure for the design of agents utilizing BPs as a targeting ligand, including the tether length between the BP and payload, the size of the payload, the number of BP ligands per payload, cleavable tethers between the BP and payload, conjugation of BPs to the payload, and comparison between BPs and other mineral targeting ligands.

5.1. Tether length

The tether length is the length of the molecular linker or spacer between the BP molecule and payload, but not necessarily the physical distance between the two, as linkers tend to be flexible molecules. Longer tether lengths are thought to reduce steric hindrance between the payload and targeting ligand enabling greater binding affinity, as the targeting ligand is free to interact with the intended surface. However, studies have demonstrated that a shorter tether length between BPs and a protein resulted in greater binding to hydroxyapatite *in vitro* [183] and *in vivo* [184]. This apparent paradox was explained in a review by Zhang et al. [86] by (1) a greater local concentration of BPs per payload as a shorter tether length reduces the spacing between BPs, (2) non-specific interactions between the protein itself and hydroxyapatite, and (3) possible electrostatic or hydrophobic interactions between the tether and hydroxyapatite. Another group reported no effect of the tether length for an amine terminated R_2 side group on binding to hydroxyapatite *in vitro* when no protein was attached [53], but all the investigated tether lengths exhibited a greater binding affinity compared with unmodified BP suggesting that an increased tether length promoted interactions of the R_2 side group with the hydroxyapatite surface (*cf.*, Fig. 3c.). The same group also demonstrated no effect of tether length on binding to hydroxyapatite *in vitro* when the protein was attached [79]. Therefore, the effect of the tether length on the binding affinity of BP-protein conjugates is not yet clear and must be determined for new BP-protein conjugates.

The tether length of a polyethylene glycol (PEG) spacer between polymer nanoparticles and BP has been shown to affect the binding affinity to hydroxyapatite *in vitro* [129]. A PEG spacer with a molecular weight of 2000 Da exhibited lower binding to hydroxyapatite compared with 550 and 750 Da, which was attributed to folding of the longer chains inhibiting interaction between the BP and hydroxyapatite [129]. Interestingly, unpublished data in our lab has indicated BP-PEG-conjugated gold nanoparticles with a PEG spacer molecular weight of 2000 Da resulted in greater binding to hydroxyapatite *in vitro* compared with 1000 or 5000 Da. Therefore, the effect of the tether length on the binding affinity of BP-nanoparticle conjugates is also not yet clear and must be determined for new BP-nanoparticle conjugates.

5.2. Size of the payload

The size of the payload is well-known to affect the biodistribution and accumulation of BP conjugates *in vivo*, especially after intravenous administration. In order to reach active bone forming units within cortical or trabecular bone after systemic intravenous delivery, BP conjugates must extravasate blood vessels through capillary fenestrae, which are normally up to 60 nm in size [185,186] and up to 150 nm in size within tumors [187]. Therefore, BP conjugates should be smaller than this size for targeted delivery to bone or bone metastases [60]. BP molecules (Fig. 2), BP–radionuclide conjugates, and BP-conjugated fluorophores are well below this size. The increase in molecular weight due to a conjugated radionuclide or fluorophore was shown to slightly alter the biodistribution compared with free BPs, but delivery to bone was not hindered [65]. However, the delivery of BP-conjugated nanoparticles and macromolecules to bone may be limited by size.

BP-functionalized bovine serum albumin (BSA) nanoparticles, with a 77 nm hydrodynamic diameter, exhibited very little bone-targeting in rats after intravenous administration [60], suggesting that the nanoparticle size may have hindered delivery to bone. In contrast, BP-functionalized nanoparticles with a hydrodynamic diameter of 195 nm [107] and 115 or 170 nm [132] exhibited significant bone accumulation after intravascular administration. Note, however, that the two latter studies only reported a relative fluorescence and did not measure the concentration or percent of the initial dose that was delivered to bone. Nonetheless, the drug encapsulated within the BP-functionalized nanoparticle did induce changes in bone mass and architecture, suggesting that the nanoparticles were delivered to the skeleton [107]. Thus, the effect of BP conjugate size on delivery to bone, especially for nanoparticles and macromolecules greater than 10 nm in size, is not well understood but fundamentally important.

Targeted delivery to pathological calcifications may also be limited by blood supply to the host tissue and the ability of BP conjugates to extravasate vessels. For example, kidney stones must be targeted by agents smaller than the 5.5 nm glomerular filtration cutoff for passage through the kidneys [188]. The size of BP conjugates designed to target breast microcalcifications is currently unknown and may be dependent on the presence of a tumor with leaky vasculature. Therefore, the delivery of BP conjugates to pathological calcifications requires different design constraints compared with delivery to the skeleton. Efficient delivery to pathological calcifications may be improved by local administration [169] or tailoring the overall size of the BP conjugate to limit bone perfusion and increase blood circulation [62].

5.3. Number of BP ligands per payload

An increased number of BP ligands per payload has been demonstrated to promote greater binding affinity to hydroxyapatite in numerous *in vitro* studies [42,43,45,62,107,125,189], but *in vivo* studies have reported varying results [43,62]. The amount of alendronate conjugated to an HPMA copolymer did not result in differences in skeletal accumulation at any time point after intravascular injection [62]. In contrast, a dendritic tetra(bisphosphonic acid) molecule conjugated to BSA

exhibited greater skeletal accumulation compared with a similar complex with fewer BP groups per BSA, but the measured difference in BPs per BSA was small suggesting that other factors may have contributed to the differences in skeletal accumulation [43]. Once again, the effect of the number of BP ligands per payload on binding affinity to hydroxyapatite is not well understood and warrants further investigation. Characterization of ligand density on nanoparticles and macromolecules can be challenging but, by way of example, methods have been developed for measuring the surface density of BPs on gold nanoparticles [42].

5.4. Cleavable tethers

Cleavable molecular tethers between the BP molecule and payload are intended to be stable during delivery and then labile after the BP binds to the mineral to enable local release of the payload [53]. Therefore, molecular linkages are designed to be cleavable under physiological conditions that are specific to the targeted site of interest. Examples include a pH-triggered linkage that is labile at low pH, such as in areas of bone resorption or fracture healing [53], or a disulfide linkage that is cleavable in the presence of thiols [44,190,191]. Simpler methods include designing a hydrolyzable molecular linker that degrades slowly *in vivo* [99]. However, this method requires that the degradation rate is carefully controlled to be longer than the circulation time in order to deliver the agent to the bone before being degraded. The release of a chemotherapy drug from a BP molecule by hydrolysis of a cleavable tether exhibited a half-life of 40 h *in vitro* [99]. Whether or not this half-life is suitable for *in vivo* delivery to bone is not known. Overall, cleavable molecular tethers are a nascent but promising strategy for the targeted delivery of drugs to bone and pathological calcifications using BP ligands.

5.5. Conjugation scheme

The methods used to conjugate BP molecules to the payload must neither alter the activity of the payload nor eliminate the binding affinity of BPs. As described above, bifunctional ligands have been designed for conjugating BPs to radionuclides to free both phosphonate groups for bone-targeting [23,136–142]. BP-radionuclide conjugates with bifunctional ligands exhibited greater binding affinity compared with traditional designs where the BP molecule acts as both the metal chelator and bone-targeting group [23,136]. In general, conjugation schemes that preserve the availability of both phosphonate groups for chelating calcium ions are necessary for maintaining a high binding affinity to mineral. Therefore, molecular linkages for conjugation should attach *via* the R_1 or R_2 side chains.

Uludag and colleagues have investigated multiple schemes for conjugating BPs to proteins [86] and polymers [121,189] for delivery to bone paying careful attention to location(s) of BP attachment to the molecular structure to maintain bioactivity. First, aminoBPs were conjugated to the lysine amino acids in BSA and shown to exhibit greater binding affinity to hydroxyapatite *in vitro* and increased bone localization *in vivo* compared with unmodified BSA [45,61]. However, this conjugation scheme attached BPs to the protein core, which was thought to negatively impact the protein bioactivity [192], although this was not investigated as BSA was just a model protein. Therefore, a new scheme was developed for conjugating BPs to carbohydrate groups, which do not play a role in the bioactivity of most proteins [192]. The carbohydrate conjugation scheme resulted in greater binding affinity to hydroxyapatite *in vitro* compared with the previous scheme using lysine amino acids [192]. However, both the carbohydrate and lysine conjugation schemes resulted in no bone binding *in vivo* while the lysine scheme with a much shorter linker did result in bone binding [184].

The preceding studies highlight that the conjugation scheme – including the conjugation chemistry, molecular length, and placement on the payload – affects the mineral binding affinity and therefore must be considered. Also, the conjugation scheme that enables the greatest binding affinity *in vitro* may not reflect the greatest binding affinity *in vivo* or may compromise bioactivity *in vivo*. Studies comparing drug activity for different conjugation schemes would provide insight into a possible design tradeoff between the binding affinity to mineral and the bioactivity of the payload. Finally, the role and relative importance of the R_1 and R_2 side groups in binding and bioactivity could be further elucidated by investigating conjugation to either separately, but to our knowledge there have been no direct comparisons of conjugation at the R_1 *versus* R_2 side groups.

6. Conclusion and future outlook

The conjugation of BP ligands to pharmaceutical drugs, including imaging probes and radiosensitizers, enables targeted delivery to bone and pathological calcifications. BPs are ideal for targeting bone due to exhibiting a high binding affinity to hydroxyapatite. One of the first clinical uses of BPs was to deliver an imaging agent (^{99}Tc-MDP) to sites of high bone turnover and BP molecules subsequently became the most widely used therapeutic in the treatment of metabolic bone diseases. No other BP conjugates have been approved for clinical use since ^{99}Tc-MDP; however, a number of BP conjugates have shown new promise to address important clinical needs. Bifunctional chelator ligands have improved the specificity of current ^{99}Tc–BP agents [138,140,142,143], which may enable lowering the administered dose and improving the safety to patients. Fluorescent BP conjugate imaging probes have been commercialized (OsteoSense™, Perkin-Elmer) and are now a widely used research tool in preclinical investigations of metabolic bone disease [147–150], bone regeneration [151], and pathological calcifications [152–154]. BP functionalized gold nanoparticles have enabled targeted delivery and contrast-enhanced X-ray detection of breast microcalcifications within murine mammary tissues [169], which may translate to improving the sensitivity and specificity of mammography for detecting breast cancer, especially in women with dense breast tissue [170]. The conjugation of BP ligands to chemotherapy agents has enabled targeted delivery of a greater dose of pharmaceutical to bone tissue while reducing detrimental off-target side-effects [96,109], which may improve the efficacy of cancer therapeutics in the treatment of bone cancer and metastases. The successful clinical translation of these and other promising new BP conjugates will require several important directions of scientific inquiry to determine (1) the pharmacological activity of both the conjugate and BP in appropriate preclinical models, (2) the minimum required dose, and (3) the most effective delivery route (*e.g.*, oral *vs.* intravenous), among others. This review attempted to highlight the wide-range of agents that can be conjugated to BPs for targeted delivery and gaps in our knowledge of fundamental structure-function relationships. Future efforts should therefore focus on closing the knowledge gaps and translating BP conjugates as new pharmaceutical drugs for targeting bone and mineral deposits.

Acknowledgments

This review was completed with support from the National Science Foundation (DMR-1309587), St. Joseph Regional Medical Center, and Walther Cancer Foundation. The authors gratefully acknowledge Dr. Elena Aikawa (Brigham and Women's Hospital, Boston, MA) and Dr. Philip Blower (Kings College London, UK) for providing the NIR fluorescence and SPECT images, respectively, of vascular calcifications targeted by a BP conjugated contrast agents in Fig. 6a.

References

[1] G.A. Rodan, T.J. Martin, Therapeutic approaches to bone diseases, Science 289 (2000) 1508–1514, http://dx.doi.org/10.1126/science.289.5484.1508.
[2] T.M. Doherty, K. Asotra, L.A. Fitzpatrick, J.-H. Qiao, D.J. Wilkin, R.C. Detrano, et al., Calcification in atherosclerosis: bone biology and chronic inflammation at the

arterial crossroads, Proc. Natl. Acad. Sci. U. S. A. 100 (2003) 11201–11206, http://dx.doi.org/10.1073/pnas.1932554100.
[3] L. Wexler, B. Brundage, J. Crouse, R. Detrano, V. Fuster, J. Maddahi, et al., Coronary artery calcification: pathophysiology, epidemiology, imaging methods, and clinical implications: a statement for health professionals from the American Heart Association, Circulation 94 (1996) 1175–1192, http://dx.doi.org/10.1161/01.cir.94.5.1175.
[4] N. Alexopoulos, P. Raggi, Calcification in atherosclerosis, Nat. Rev. Cardiol. 6 (2009) 681–688, http://dx.doi.org/10.1038/nrcardio.2009.165.
[5] M.P. Morgan, M.M. Cooke, G.M. McCarthy, Microcalcifications associated with breast cancer: an epiphenomenon or biologically significant feature of selected tumors? J. Mammary Gland Biol. Neoplasia 10 (2005) 181–187, http://dx.doi.org/10.1007/s10911-005-5400-6.
[6] H. Xu, A.L. Zisman, F.L. Coe, E.M. Worcester, Kidney stones: an update on current pharmacological management and future directions, Expert. Opin. Pharmacother. 14 (2013) 435–447, http://dx.doi.org/10.1517/14656566.2013.775250.
[7] R.G.G. Russell, Bisphosphonates: the first 40 years, Bone 49 (2011) 2–19, http://dx.doi.org/10.1016/j.bone.2011.04.022.
[8] H. Fleisch, Bisphosphonates: mechanisms of action, Endocr. Rev. 19 (1998) 80–100.
[9] H. Fleisch, R.G.G. Russell, S. Bisaz, P.A. Casey, R.C. Muhlbauer, The influence of pyrophosphate analogues (diphosphonates) on the precipitation and dissolution of calcium phosphate *in vitro* and *in vivo*, Calcif. Tissue Res. 2 (1968) 10, http://dx.doi.org/10.1007/BF02065192.
[10] M.D. Francis, R.G.G. Russell, H. Fleisch, Disphosphonates inhibit formation of calcium phosphate crystals in vitro and pathological calcification *in vivo*, Science 165 (1969) 1264–1266.
[11] G.H. Nancollas, R. Tang, R.J. Phipps, Z. Henneman, S. Gulde, W. Wu, et al., Novel insights into actions of bisphosphonates on bone: differences in interactions with hydroxyapatite, Bone 38 (2006) 617–627, http://dx.doi.org/10.1016/j.bone.2005.05.003.
[12] H. Fleisch, H. Fleisch, R.G.G. Russell, R.G.G. Russell, M.D. Francis, M.D. Francis, Diphosphonates inhibit hydroxyapatite dissolution *in vitro* and bone resorption in tissue culture and *in vivo*, Science 165 (1969) 1262–1264, http://dx.doi.org/10.1126/science.165.3899.1262.
[13] C.A.L. Bassett, A. Donath, F. Macagno, R. Preisig, H. Fleisch, M.D. Francis, Disphosphonates in the treatment of myositis ossificans, Lancet 294 (1969) 845, http://dx.doi.org/10.1016/S0140-6736(69)92295-8.
[14] J.M. Baumann, S. Bisaz, H. Fleisch, M. Wacker, Biochemical and clinical effects of ethane-1-hydroxy-1,1-diphosphonate in calcium nephrolithiasis, Clin. Sci. Mol. Med. 54 (1978) 509–516.
[15] I. Fogelman, R.G. Bassent, J.G. Turner, D.L. Citrin, I.T. Boyle, W.R. Greig, The use of whole-body retention of Tc-99m disphosphonate in the diagnosis of metabolic bone disease, J. Nucl. Med. 19 (1978) 270–275.
[16] D.K. Wysowski, P. Greene, Trends in osteoporosis treatment with oral and intravenous bisphosphonates in the United States, 2002–2012, Bone 57 (2013) 423–428, http://dx.doi.org/10.1016/j.bone.2013.09.008.
[17] M. Pazianas, B. Abrahamsen, Safety of bisphosphonates, Bone 49 (2011) 103–110, http://dx.doi.org/10.1016/j.bone.2011.01.003.
[18] F.H. Ebetino, A.-M.L. Hogan, S. Sun, M.K. Tsoumpra, X. Duan, J.T. Triffitt, et al., The relationship between the chemistry and biological activity of the bisphosphonates, Bone 49 (2011) 20–33, http://dx.doi.org/10.1016/j.bone.2011.03.774.
[19] A.M. Flanagan, T.J. Chambers, Dichloromethylenebiphosphonate (Cl2MBP) inhibits bone resorption through injury to osteoclasts that resorb Cl2MBP-coated bone, Bone 6 (1989) 33–43.
[20] M. Ito, M. Chokki, O.Y.Y. Satomi, Y. Azuma, T. Ohta, et al., Comparison of the cytotoxic effects of bisphosphonate *in vitro* and *in vivo*, Calcif. Tissue Int. 63 (1998) 143–147.
[21] D.E. Hughes, K.R. Wright, H.L. Uy, A. Sasaki, T. Yoneda, G.D. Roodman, et al., Bisphosphonates promote apoptosis in murine osteoclasts *in vitro* and *in vivo*, J. Bone Miner. Res. 10 (1995) 1478–1487, http://dx.doi.org/10.1002/jbmr.5650101008.
[22] E.M. Lewiecki, Safety of long-term bisphosphonate therapy for the management of osteoporosis, Drugs 71 (2011) 791–814, http://dx.doi.org/10.2165/11585470-000000000-00000.
[23] R. Torres Martin de Rosales, C. Finucane, S.J. Mather, P.J. Blower, Bifunctional bisphosphonate complexes for the diagnosis and therapy of bone metastases, Chem. Commun. (2009) 4847–4849, http://dx.doi.org/10.1039/b908652h.
[24] H. Hyun, H. Wada, K. Bao, J. Gravier, Y. Yadav, M. Laramie, et al., Phosphonated near-infrared fluorophores for biomedical imaging of bone, Angew. Chem. Int. Ed. 53 (2014) 10668–10672, http://dx.doi.org/10.1002/anie.201404930.
[25] A. Zaheer, R.E. Lenkinski, A. Mahmood, A.G. Jones, L.C. Cantley, J.V. Frangioni, *In vivo* near-infrared fluorescence imaging of osteoblastic activity, Nat. Biotechnol. 19 (2001) 1148–1154, http://dx.doi.org/10.1038/nbt1201-1148.
[26] R.E. Lenkinski, M. Ahmed, A. Zaheer, J.V. Frangioni, S.N. Goldberg, Near-infrared fluorescence imaging of microcalcification in an animal model of breast cancer, Acad. Radiol. 10 (2003) 1159–1164, http://dx.doi.org/10.1016/S1076-6332(03)00253-8.
[27] R.G.G. Russell, N.B. Watts, F.H. Ebetino, M.J. Rogers, Mechanisms of action of bisphosphonates: similarities and differences and their potential influence on clinical efficacy, Osteoporos. Int. 19 (2008) 733–759, http://dx.doi.org/10.1007/s00198-007-0540-8.
[28] K.R. Bhushan, P. Misra, F. Liu, S. Mathur, R.E. Lenkinski, J.V. Frangioni, Detection of breast cancer microcalcifications using a dual-modality SPECT/NIR fluorescent probe, J. Am. Chem. Soc. 130 (2008) 17648–17649, http://dx.doi.org/10.1021/ja807099s.
[29] E. van Beek, M. Hoekstra, M. Van de Ruit, C. Lowik, S. Papapoulos, Structural requirements for bisphosphonate actions *in vitro*, J. Bone Miner. Res. 9 (1994) 1875–1882, http://dx.doi.org/10.1002/jbmr.5650091206.
[30] F.H. Ebetino, B.L. Barnett, R.G.G. Russell. A computational model delineates differences in hydroxyapatite binding affinities of bisphosphonate [abstract]. J. Bone Miner. Res. 20 [Suppl 1], 2005, S259. http://dx.doi.org/10.1002/jbmr.5650201305.
[31] R. Fujisawa, Y. Kuboki, Preferential adsorption of dentin and bone acidic proteins on the (100) face of hydroxyapatite crystals, Biochim. Biophys. Acta 1075 (1991) 56–60, http://dx.doi.org/10.1016/0304-4165(91)90074-Q.
[32] J. Moradian-Oldak, F. Frolow, L. Addadi, S. Weiner, Interaction between acidic matrix macromolecules and calcium phosphate ester crystals: relevance to carbonate apatite formation in biomineralization, Proc. Biol. Sci. 247 (1992) 47–55.
[33] L. Addadi, S. Weiner, Interactions between acidic proteins and crystals: stereochemical requirements in biomineralization, Proc. Natl. Acad. Sci. U. S. A. 82 (1985) 4110–4114.
[34] R. Fujisawa, Y. Wada, Y. Nodasaka, Y. Kuboki, Acidic amino acid-rich sequences as binding sites of osteonectin to hydroxyapatite crystals, Biochim. Biophys. Acta 1292 (1996) 53–60, http://dx.doi.org/10.1016/0167-4838(95)00190-5.
[35] S. Kasugai, R. Fujisawa, Y. Waki, K. Miyamoto, K. Ohya, Selective drug delivery system to bone: small peptide (Asp)(6) conjugation, J. Bone Miner. Res. 15 (2000) 936–943, http://dx.doi.org/10.1359/jbmr.2000.15.5.936.
[36] M.B. Murphy, J.D. Hartgerink, A. Goepferich, A.G. Mikos, Synthesis and *in vitro* hydroxyapatite binding of peptides conjugated to calcium-binding moieties, Biomacromolecules 8 (2007) 2237–2243, http://dx.doi.org/10.1021/bm070121s.
[37] D. Wang, S. Miller, M. Sima, P. Kopecková, J. Kopecek, Synthesis and evaluation of water-soluble polymeric bone-targeted drug delivery systems, Bioconjug. Chem. 14 (2003) 853–859, http://dx.doi.org/10.1021/bc034090j.
[38] R.D. Ross, R.K. Roeder, Binding affinity of surface functionalized gold nanoparticles to hydroxyapatite, J. Biomed. Mater. Res. 99A (2011) 58–66, http://dx.doi.org/10.1002/jbm.a.33165.
[39] R.D. Ross, L.E. Cole, R.K. Roeder, Relative binding affinity of carboxylate-, phosphonate-, and bisphosphonate-functionalized gold nanoparticles targeted to damaged bone tissue, J. Nanoparticle Res. 14 (2012) 1175, http://dx.doi.org/10.1007/s11051-012-1175-z.
[40] D.G. Kinniburgh, General purpose adsorption isotherms, Environ. Sci. Technol. 20 (1986) 895–904, http://dx.doi.org/10.1021/es00151a008.
[41] T. Vitha, V. Kubícek, P. Hermann, Z.I. Kolar, H.T. Wolterbeek, J.A. Peters, et al., Complexes of DOTA-bisphosphonate conjugates: probes for determination of adsorption capacity and affinity constants of hydroxyapatite, Langmuir 24 (2008) 1952–1958, http://dx.doi.org/10.1021/la702753j.
[42] R.D. Ross, L.E. Cole, J.M.R. Tilley, R.K. Roeder, Effects of functionalized gold nanoparticle size on X-ray attenuation and substrate binding affinity, Chem. Mater. 26 (2014) 1187–1194, http://dx.doi.org/10.1021/cm4035616.
[43] G. Bansal, J.E.I. Wright, C. Kucharski, H. Uluda, A dendritic tetra(bisphosphonic acid) for improved targeting of proteins to bone, Angew. Chem. Int. Ed. 44 (2005) 3710–3714, http://dx.doi.org/10.1002/anie.200500350.
[44] J.E.I. Wright, S.A. Gittens, G. Bansal, P.I. Kitov, D. Sindrey, C. Kucharski, et al., A comparison of mineral affinity of bisphosphonate–protein conjugates constructed with disulfide and thioether linkages, Biomaterials 27 (2006) 769–784, http://dx.doi.org/10.1016/j.biomaterials.2005.06.012.
[45] H. Uludag, N. Kousinioris, T. Gao, D. Kantoci, Bisphosphonate conjugation to proteins as a means to impart bone affinity, Biotechnol. Prog. 16 (2000) 258–267, http://dx.doi.org/10.1021/bp990154m.
[46] G. Bansal, S.B.A. Gittens, H. Uludag, A di(bisphosphonic acid) for protein coupling and targeting to bone, J. Pharm. Sci. 93 (2004) 2788–2799, http://dx.doi.org/10.1002/jps.20186.
[47] Y. Yang, K.H. Bhandari, A. Panahifar, M.R. Doschak, Synthesis, characterization and biodistribution studies of ^{125}I-radioiodinated di-PEGylated bone targeting salmon calcitonin analogue in healthy rats, Pharm. Res. 31 (2013) 1146–1157, http://dx.doi.org/10.1007/s11095-013-1237-7.
[48] M.R. Doschak, C.M. Kucharski, J.E.I. Wright, R.F. Zernicke, H. Uludag, Improved bone delivery of osteoprotegerin by bisphosphonate conjugation in a rat model of osteoarthritis, Mol. Pharm. 6 (2009) 634–640, http://dx.doi.org/10.1021/mp8002368.
[49] A.A. El-Mabhouh, C.A. Angelov, R. Cavell, J.R. Mercer, A ^{99m}Tc-labeled gemcitabine bisphosphonate drug conjugate as a probe to assess the potential for targeted chemotherapy of metastatic bone cancer, Nucl. Med. Biol. 33 (2006) 715–722, http://dx.doi.org/10.1016/j.nucmedbio.2006.06.004.
[50] C. Rill, Z.I. Kolar, G. Kickelbick, H.T. Wolterbeek, J.A. Peters, Kinetics and thermodynamics of adsorption on hydroxyapatite of the [^{160}Tb]terbium complexes of the bone-targeting ligands DOTP and BPPED, Langmuir 25 (2009) 2294–2301, http://dx.doi.org/10.1021/la803562e.
[51] G.M.S. Zayed, J.K.V. Tessmar, Heterobifunctional poly(ethylene glycol) derivatives for the surface modification of gold nanoparticles toward bone mineral targeting, Macromol. Biosci. 12 (2012) 1124–1136, http://dx.doi.org/10.1002/mabi.201200046.
[52] Z.J. Henneman, G.H. Nancollas, F.H. Ebetino, R.G.G. Russell, R.J. Phipps, Bisphosphonate binding affinity as assessed by inhibition of carbonated apatite dissolution *in vitro*, J. Biomed. Mater. Res. 85A (2008) 993–1000, http://dx.doi.org/10.1002/jbm.a.31599.
[53] J.N. Yewle, D.A. Puleo, L.G. Bachas, Enhanced affinity bifunctional bisphosphonates for targeted delivery of therapeutic agents to bone, Bioconjug. Chem. 22 (2011) 2496–2506, http://dx.doi.org/10.1021/bc2003132.
[54] P. Koutsoukos, Z. Amjad, M.B. Tomson, G.H. Nancollas, Crystallization of calcium phosphates. A constant composition study, J. Am. Chem. Soc. 102 (1980) 1553–1557, http://dx.doi.org/10.1021/ja00525a015.

[55] S. Mukherjee, Y. Song, E. Oldfield, NMR investigations of the static and dynamic structures of bisphosphonates on human bone. A molecular model, J. Am. Chem. Soc. 130 (2008) 1264–1273, http://dx.doi.org/10.1021/ja0759949.
[56] W. Jahnke, C. Henry, An *in vitro* assay to measure targeted drug delivery to bone mineral, ChemMedChem 5 (2010) 770–776, http://dx.doi.org/10.1002/cmdc.201000016.
[57] C.-T. Leu, E. Luegmayr, L.P. Freedman, G.A. Rodan, A.A. Reszka, Relative binding affinities of bisphosphonates for human bone and relationship to antiresorptive efficacy, Bone 38 (2006) 628–636, http://dx.doi.org/10.1016/j.bone.2005.07.023.
[58] M.A. Lawson, Z. Xia, B.L. Barnett, J.T. Triffitt, R.J. Phipps, J.E. Dunford, et al., Differences between bisphosphonates in binding affinities for hydroxyapatite, J. Biomed. Mater. Res. 92B (2010) 149–155, http://dx.doi.org/10.1002/jbm.b.31500.
[59] H. Uludag, Bisphosphonates as a foundation of drug delivery to bone, Curr. Pharm. Des. 8 (2002) 1929–1944, http://dx.doi.org/10.2174/12812023393585.
[60] G. Wang, C. Kucharski, X. Lin, H. Uludag, Bisphosphonate-coated BSA nanoparticles lack bone targeting after systemic administration, J. Drug Target. 18 (2010) 611–626, http://dx.doi.org/10.3109/10611861003622560.
[61] H. Uludag, J. Yang, Targeting systemically administered proteins to bone by bisphosphonate conjugation, Biotechnol. Prog. 18 (2002) 604–611, http://dx.doi.org/10.1021/bp0200447.
[62] H. Pan, M. Sima, P. Kopecková, K. Wu, S. Gao, J. Liu, et al., Biodistribution and pharmacokinetic studies of bone-targeting N-(2-hydroxypropyl)methacrylamide copolymer–alendronate conjugates, Mol. Pharm. 5 (2008) 548–558, http://dx.doi.org/10.1021/mp800003u.
[63] A.J. Roelofs, C.A. Stewart, S. Sun, K.M. Biazewska, B.A. Kashemirov, C.E. McKenna, et al., Influence of bone affinity on the skeletal distribution of fluorescently labeled bisphosphonates *in vivo*, J. Bone Miner. Res. 27 (2012) 835–847, http://dx.doi.org/10.1002/jbmr.1543.
[64] J.H. Lin, Bisphosphonates: a review of their pharmacokinetic properties, Bone 18 (1996) 74–85, http://dx.doi.org/10.1016/8756-3282(95)00445-9.
[65] S. Cremers, S. Papapoulos, Pharmacology of bisphosphonates, Bone 49 (2011) 42–49, http://dx.doi.org/10.1016/j.bone.2011.01.014.
[66] S.T. Harris, N.B. Watts, H.K. Genant, C.D. McKeever, Effects of risedronate treatment on vertebral and nonvertebral fractures in women with postmenopausal osteoporosis: a randomized controlled trial, J. Am. Med. Assoc. 282 (1999) 1344–1352, http://dx.doi.org/10.1001/jama.282.14.1344.
[67] R. Eastell, J.S. Walsh, N.B. Watts, E. Siris, Bisphosphonates for postmenopausal osteoporosis, Bone 49 (2011) 82–88, http://dx.doi.org/10.1016/j.bone.2011.02.011.
[68] P.D. Delmas, Treatment of postmenopausal osteoporosis, Lancet 359 (2002) 2018–2026, http://dx.doi.org/10.1016/S0140-6736(02)08827-X.
[69] E.F. Eriksen, A. Díez-Pérez, S. Boonen, Update on long-term treatment with bisphosphonates for postmenopausal osteoporosis: a systematic review, Bone 58 (2014) 126–135, http://dx.doi.org/10.1016/j.bone.2013.09.023.
[70] B.L. Riggs, L.J. Melton, The prevention and treatment of osteoporosis, New Engl. J. Med. 327 (1992) 620–627.
[71] F. Bauss, A. Esswein, K. Reiff, G. Sponer, B. Müller-Beckmann, Effect of 17β-estradiol-bisphosphonate conjugates, potential bone-seeking estrogen pro-drugs, on 17β-estradiol serum kinetics and bone mass in rats, Calcif. Tissue Int. 59 (1996) 168–173.
[72] J. Fujisaki, Y. Tokunaga, T. Takashashi, S. Kimura, F. Shimojo, T. Hata, Osteotropic drug delivery system (ODDS) based on bisphosphonic prodrug. Biological disposition and targeting characteristics of osteotropic estradiol, Biol. Pharm. Bull. 20 (1997) 1183–1187, http://dx.doi.org/10.1248/bpb.20.1183.
[73] J. Fujisaki, Y. Tokunaga, T. Takashashi, F. Shimojo, S. Kimura, T. Hata, Osteotropic drug delivery system (ODDS) based on bisphosphonic prodrug. I.V. Effects of osteotropic estradiol on bone mineral density and uterine weight in ovariectomized rats, J. Drug Target. 5 (1998) 129–138, http://dx.doi.org/10.3109/10611869808995866.
[74] P.C.B. Page, M.J. McKenzie, J.A. Gallagher, Novel synthesis of bis(phosphonic acid)-steroid conjugates, J. Org. Chem. 66 (2001) 3704–3708, http://dx.doi.org/10.1021/jo001489h.
[75] P.C.B. Page, J.P.G. Moore, I. Mansfield, M.J. McKenzie, W.B. Bowler, J.A. Gallagher, Synthesis of bone-targeted oestrogenic compounds for the inhibition of bone resorption, Tetrahedron 57 (2001) 1837–1847, http://dx.doi.org/10.1016/S0040-4020(00)01164-9.
[76] M. Morioka, A. Kamizono, H. Takikawa, A. Mori, H. Ueno, S.-I. Kadowaki, et al., Design, synthesis, and biological evaluation of novel estradiol-bisphosphonate conjugates as bone-specific estrogens, Bioorg. Med. Chem. 18 (2010) 1143–1148, http://dx.doi.org/10.1016/j.bmc.2009.12.041.
[77] L. Gil, Y. Han, E.E. Opas, G.A. Rodan, R. Ruel, J.G. Seedor, et al., Prostaglandin E2-bisphosphonate conjugates: potential agents for treatment of osteoporosis, Bioorg. Med. Chem. 7 (1999) 901–919, http://dx.doi.org/10.1016/S0968-0896(99)00045-0.
[78] S. Arns, R. Gibe, A. Moreau, M.M. Morshed, R.N. Young, Design and synthesis of novel bone-targeting dual-action pro-drugs for the treatment and reversal of osteoporosis, Bioorg. Med. Chem. 20 (2012) 2131–2140, http://dx.doi.org/10.1016/j.bmc.2012.01.024.
[79] J.N. Yewle, D.A. Puleo, L.G. Bachas, Bifunctional bisphosphonate for delivering PTH(1-34) to bone mineral with enhanced bioactivity, Biomaterials 34 (2013) 3141–3149, http://dx.doi.org/10.1016/j.biomaterials.2013.01.059.
[80] M. Li, D.D. Thompson, V.M. Paralkar, Prostaglandin E2 receptors in bone formation, Int. Orthop. 31 (2007) 767–772, http://dx.doi.org/10.1007/s00264-007-0406-x.
[81] K.H. Bhandari, M. Newa, H. Uludag, M.R. Doschak, Synthesis, characterization and *in vitro* evaluation of a bone targeting delivery system for salmon calcitonin, Int. J. Pharm. 394 (2010) 26–34, http://dx.doi.org/10.1016/j.ijpharm.2010.04.015.
[82] Y.-H. Lee, P.J. Sinko, Oral delivery of salmon calcitonin, Adv. Drug Deliv. Rev. 42 (2000) 225–238, http://dx.doi.org/10.1016/S0169-409X(00)00063-6.
[83] D. Naot, J. Cornish, The role of peptides and receptors of the calcitonin family in the regulation of bone metabolism, Bone 1–6 (2008)http://dx.doi.org/10.1016/j.bone.2008.07.003.
[84] K.H. Bhandari, M. Newa, J. Chapman, M.R. Doschak, Synthesis, characterization and evaluation of bone targeting salmon calcitonin analogs in normal and osteoporotic rats, J. Control. Release 158 (2012) 44–52, http://dx.doi.org/10.1016/j.jconrel.2011.09.096.
[85] S. Gittens, G. Bansal, R. Zernicke, H. Uludag, Designing proteins for bone targeting, Adv. Drug Deliv. Rev. 57 (2005) 1011–1036, http://dx.doi.org/10.1016/j.addr.2004.12.015.
[86] S. Zhang, G. Gangal, H. Uludag, "Magic bullets" for bone diseases: progress in rational design of bone-seeking medicinal agents, Chem. Soc. Rev. 36 (2007) 507, http://dx.doi.org/10.1039/b512310k.
[87] R.E. Coleman, Clinical features of metastatic bone disease and risk of skeletal morbidity, Clin. Cancer Res. 12 (2006) 6243s–6249s, http://dx.doi.org/10.1158/1078-0432.CCR-06-0931.
[88] G.R. Mundy, Metastasis to bone: causes, consequences and therapeutic opportunities, Nat. Rev. Cancer 2 (2002) 584–593, http://dx.doi.org/10.1038/nrc867.
[89] R.E. Coleman, E.V. McCloskey, Bisphosphonates in oncology, Bone 49 (2011) 71–76, http://dx.doi.org/10.1016/j.bone.2011.02.003.
[90] R.E. Coleman, Metastatic bone disease: clinical features, pathophysiology and treatment strategies, Cancer Treat. Rev. 27 (2001) 165–176, http://dx.doi.org/10.1053/ctrv.2001.0210.
[91] H.L. Neville-Webbe, M. Gnant, R.E. Coleman, Potential anticancer properties of bisphosphonates, Semin. Oncol. 37 (2010) S53–S65, http://dx.doi.org/10.1053/j.seminoncol.2010.06.008.
[92] L. Brannon-Peppas, J.O. Blanchette, Nanoparticle and targeted systems for cancer therapy, Adv. Drug Deliv. Rev. 56 (2004) 1649–1659, http://dx.doi.org/10.1016/j.addr.2004.02.014.
[93] T. Klenner, P. Valenzuela-Paz, B.K. Keppler, G. Angres, H.R. Scherf, F. Wingen, et al., Cisplatin-linked phosphonates in the treatment of the transplantable osteosarcoma *in vitro* and *in vivo*, Cancer Treat. Rev. 17 (1990) 253–259, http://dx.doi.org/10.1016/0305-7372(90)90056-L.
[94] Z. Xue, M. Lin, J. Zhu, J. Zhang, Y. Li, Z. Guo, Platinum(ii) compounds bearing bone-targeting group: synthesis, crystal structure and antitumor activity, Chem. Commun. 46 (2010) 1212, http://dx.doi.org/10.1039/b922222g.
[95] K. Miller, R. Erez, E. Segal, D. Shabat, R. Satchi-Fainaro, Targeting bone metastases with a bispecific anticancer and antiangiogenic polymer–alendronate–taxane conjugate, Angew. Chem. Int. Ed. 48 (2009) 2949–2954, http://dx.doi.org/10.1002/anie.200805133.
[96] K. Miller, A. Eldar-Boock, D. Polyak, E. Segal, L. Benayoun, Y. Shaked, et al., Antiangiogenic antitumor activity of HPMA copolymer–paclitaxel–alendronate conjugate on breast cancer bone metastasis mouse model, Mol. Pharm. 8 (2011) 1052–1062, http://dx.doi.org/10.1021/mp200083n.
[97] K.R. Chaudhari, A. Kumar, V.K.M. Khandelwal, A.K. Mishra, J. Mönkkönen, R.S.R. Murthy, Targeting efficiency and biodistribution of zoledronate conjugated docetaxel loaded pegylated PBCA nanoparticles for bone metastasis, Adv. Funct. Mater. 22 (2012) 4101–4114, http://dx.doi.org/10.1002/adfm.201102357.
[98] N. Margiotta, F. Capitelli, R. Ostuni, G. Natile, A new dinuclear platinum complex with a nitrogen-containing geminal bisphosphonate as potential anticancer compound specifically targeted to bone tissue, J. Inorg. Biochem. 102 (2008) 2078–2086, http://dx.doi.org/10.1016/j.jinorgbio.2008.07.008.
[99] R. Erez, S. Ebner, B. Attali, D. Shabat, Chemotherapeutic bone-targeted bisphosphonate prodrugs with hydrolytic mode of activation, Bioorg. Med. Chem. Lett. 18 (2008) 816–820, http://dx.doi.org/10.1016/j.bmcl.2007.11.029.
[100] A.A. El-Mabhouh, J.R. Mercer, ^{188}Re-labelled gemcitabine/bisphosphonate (Gem/BP): a multi-functional, bone-specific agent as a potential treatment for bone metastases, Eur. J. Nucl. Med. Mol. Imaging 35 (2008) 1240–1248, http://dx.doi.org/10.1007/s00259-008-0728-y.
[101] A.A. El-Mabhouh, P.N. Nation, J.T. Abele, T. Riauka, E. Postema, A. McEwan, et al., A conjugate of gemcitabine with bisphosphonate (Gem/BP) showed potential as a targeted bone-specific therapeutic agent in an animal model of human breast cancer metastases, Oncol. Res. 19 (2011) 287–295, http://dx.doi.org/10.3727/096504011X13021877989874.
[102] A.A. El-Mabhouh, C.A. Angelov, A. McEwan, G. Jia, J.R. Mercer, Preclinical investigations of drug and radionuclide conjugates of bisphosphonates for the treatment of metastatic bone cancer, Cancer Biother. Radiopharm. 19 (2014) 627–640, http://dx.doi.org/10.1089/cbr.2004.19.627.
[103] O. Fabulet, G. Sturtz, Synthesis of gem-bisphosphonic doxorubicin conjugates, Phosphorus Sulfur Silicon Relat. Elem. 101 (1995) 225–234, http://dx.doi.org/10.1080/10426509508042521.
[104] K. Hochdörffer, K. Abu Ajaj, C. Schäfer-Obodozie, F. Kratz, Development of novel bisphosphonate prodrugs of doxorubicin for targeting bone metastases that are cleaved pH dependently or by cathepsin B: Synthesis, cleavage properties, and binding properties to hydroxyapatite as well as bone matrix, J. Med. Chem. 55 (2012) 7502–7515, http://dx.doi.org/10.1021/jm300493m.
[105] F. Hosain, R.P. Spencer, H.M. Couthon, G.L. Sturtz, Targeted delivery of antineoplastic agent to bone: Biodistribution studies of technetium-99m-labeled gem-bisphosphonate conjugate of methotrexate, J. Nucl. Med. 37 (1996) 105–107.
[106] J.K. Agyin, B. Santhamma, S.S. Roy, Design, synthesis, and biological evaluation of bone-targeting proteasome inhibitors for multiple myeloma, Bioorg. Med. Chem. Lett. 23 (2013) 6455–6458, http://dx.doi.org/10.1016/j.bmcl.2013.09.043.
[107] A. Swami, M.R. Reagan, P. Basto, Y. Mishima, N. Kamaly, S. Glavey, et al., Engineered nanomedicine for myeloma and bone microenvironment targeting, Proc. Natl. Acad. Sci. U. S. A. 111 (2014) 10287–10292, http://dx.doi.org/10.1073/pnas.1401337111.

[108] M.M. Reinholz, S.P. Zinnen, A.C. Dueck, D. Dingli, G.G. Reinholz, L.A. Jonart, et al., A promising approach for treatment of tumor-induced bone diseases: utilizing bisphosphonate derivatives of nucleoside antimetabolites, Bone 47 (2010) 12–22, http://dx.doi.org/10.1016/j.bone.2010.03.006.
[109] E. Segal, H. Pan, L. Benayoun, P. Kopecková, Y. Shaked, J. Kopecek, et al., Enhanced anti-tumor activity and safety profile of targeted nano-scaled HPMA copolymer–alendronate–TNP-470 conjugate in the treatment of bone malignances, Biomaterials 32 (2011) 4450–4463, http://dx.doi.org/10.1016/j.biomaterials.2011.02.059.
[110] D.P. Lew, F.A. Waldvogel, Osteomyelitis, Lancet 364 (2004) 369–379, http://dx.doi.org/10.1016/S0140-6736(04)16727-5.
[111] E. Romas, Bone loss in inflammatory arthritis: mechanisms and therapeutic approaches with bisphosphonates, Best Pract. Res. Clin. Rheumatol. 19 (2005) 1065–1079, http://dx.doi.org/10.1016/j.berh.2005.06.008.
[112] K.S.E. Tanaka, E. Dietrich, S. Ciblat, C. Métayer, F.F. Arhin, I. Sarmiento, et al., Synthesis and in vitro evaluation of bisphosphonated glycopeptides for the treatment of osteomyelitis, Bioorg. Med. Chem. Lett. 20 (2010) 1355–1359, http://dx.doi.org/10.1016/j.bmcl.2010.01.006.
[113] P. Herczegh, T.B. Buxton, J.C. McPherson, Á. Kovács-Kulyassa, P.D. Brewer, F. Sztaricskai, et al., Osteoadsorptive bisphosphonate derivatives of fluoroquinolone antibacterials, J. Med. Chem. 45 (2002) 2338–2341, http://dx.doi.org/10.1021/jm0105326.
[114] T.J. Houghton, K.S.E. Tanaka, T. Kang, E. Dietrich, Y. Lafontaine, D. Delorme, et al., Linking bisphosphonates to the free amino groups in fluoroquinolones: preparation of osteotropic prodrugs for the prevention of osteomyelitis, J. Med. Chem. 51 (2008) 6955–6969, http://dx.doi.org/10.1021/jm801007z.
[115] R. Altman, B. Bosch, K. Brune, P. Patrignani, C. Young, Advances in NSAID development: evolution of diclofenac products using pharmaceutical technology, Drugs 75 (2015) 859–877, http://dx.doi.org/10.1007/s40265-015-0392-z.
[116] H. Hirabayashi, T. Takahashi, J. Fujisaki, T. Masunaga, S. Sato, J. Hiroi, et al., Bone-specific delivery and sustained release of diclofenac, a non-steroidal anti-inflammatory drug, via bisphosphonic prodrug based on the Osteotropic Drug Delivery System (ODDS), J. Control. Release 70 (2001) 183–191, http://dx.doi.org/10.1016/S0168-3659(00)00355-2.
[117] H. Hirabayashi, T. Sawamoto, J. Fujisaki, Y. Tokunaga, S. Kimura, T. Hata, Dose-dependent pharmacokinetics and disposition of bisphosphonic prodrug of diclofenac based on osteotropic drug delivery system (ODDS), Biopharm. Drug Dispos. 23 (2002) 307–315, http://dx.doi.org/10.1002/bdd.323.
[118] M.L. Young, D.G. Little, H.K.W. Kim, Evidence for using bisphosphonate to treat Legg-Calvé-Perthes disease, Clin. Orthop. Relat. Res. 470 (2012) 2462–2475, http://dx.doi.org/10.1007/s11999-011-2240-0.
[119] F. Fanord, K. Fairbairn, H. Kim, A. Garces, V. Bhethanabotla, V.K. Gupta, Bisphosphonate-modified gold nanoparticles: a useful vehicle to study the treatment of osteonecrosis of the femoral head, Nanotechnology 22 (2010) 035102, http://dx.doi.org/10.1088/0957-4484/22/3/035102.
[120] H. Katsumi, M. Takashima, J.-I. Sano, K. Nishiyama, N. Kitamura, T. Sakane, et al., Development of polyethylene glycol-conjugated alendronate, a novel nitrogen-containing bisphosphonate derivative: evaluation of absorption, safety, and effects after intrapulmonary administration in rats, J. Pharm. Sci. 100 (2011) 3783–3792, http://dx.doi.org/10.1002/jps.22620.
[121] S. Zhang, J.E.I. Wright, N. Özber, H. Uludag, The interaction of cationic polymers and their bisphosphonate derivatives with hydroxyapatite, Macromol. Biosci. 7 (2007) 656–670, http://dx.doi.org/10.1002/mabi.200600286.
[122] L. de Miguel, M. Noiray, G. Surpateanu, B.I. Iorga, G. Ponchel, Poly(y-benzyl-L-glutamate)-PEG-alendronate multivalent nanoparticles for bone targeting, Int. J. Pharm. 460 (2014) 73–82, http://dx.doi.org/10.1016/j.ijpharm.2013.10.048.
[123] S. D'Souza, H. Murata, M.V. Jose, S. Askarova, Y. Yantsen, J.D. Andersen, et al., Engineering of cell membranes with a bisphosphonate-containing polymer using ATRP synthesis for bone targeting, Biomaterials 35 (2014) 9447–9458, http://dx.doi.org/10.1016/j.biomaterials.2014.07.041.
[124] W.H. De Jong, P.J. Borm, Drug delivery and nanoparticles: applications and hazards, Int. J. Nanomedicine 3 (2008) 133–149.
[125] V. Hengst, C. Oussoren, T. Kissel, G. Storm, Bone targeting potential of bisphosphonate-targeted liposomes. Preparation, characterization and hydroxyapatite binding *in vitro*, Int. J. Pharm. 331 (2007) 224–227, http://dx.doi.org/10.1016/j.ijpharm.2006.11.024.
[126] G. Wang, N.Z. Mostafa, V. Incani, C. Kucharski, H. Uludağ, Bisphosphonate-decorated lipid nanoparticles designed as drug carriers for bone diseases, J. Biomed. Mater. Res. 100A (2011) 684–693, http://dx.doi.org/10.1002/jbm.a.34002.
[127] G. Wang, M.E. Babadagli, H. Uludağ, Bisphosphonate-derivatized liposomes to control drug release from collagen-hydroxyapatite scaffolds, Mol. Pharm. 8 (2011) 1025–1034, http://dx.doi.org/10.1021/mp200028w.
[128] T. Anada, Y. Takeda, Y. Honda, K. Sakurai, O. Suzuki, Synthesis of calcium phosphate-binding liposome for drug delivery, Bioorg. Med. Chem. Lett. 19 (2009) 4148–4150, http://dx.doi.org/10.1016/j.bmcl.2009.05.117.
[129] S.-W. Choi, J.-H. Kim, Design of surface-modified poly(D, L-lactide-co-glycolide) nanoparticles for targeted drug delivery to bone, J. Control. Release 122 (2007) 24–30, http://dx.doi.org/10.1016/j.jconrel.2007.06.003.
[130] E. Cenni, D. Granchi, S. Avnet, C. Fotia, M. Salerno, D. Micieli, et al., Biocompatibility of poly(D, L-lactide-co-glycolide) nanoparticles conjugated with alendronate, Biomaterials 29 (2008) 1400–1411, http://dx.doi.org/10.1016/j.biomaterials.2007.12.022.
[131] E. Cenni, S. Avnet, D. Granchi, C. Fotia, M. Salerno, D. Micieli, et al., The effect of poly(D, L-lactide-co-glycolide)-alendronate conjugate nanoparticles on human osteoclast precursors, J. Biomater. Sci. Polym. Ed. 23 (2012) 1285–1300, http://dx.doi.org/10.1163/092050611X580373.
[132] S.W. Morton, N.J. Shah, M.A. Quadir, Z.J. Deng, Z. Poon, P.T. Hammond, Osteotropic therapy via targeted layer-by-layer nanoparticles, Adv. Healthcare Mater. 3 (2014) 867–875, http://dx.doi.org/10.1002/adhm.201300465.
[133] Y.-L. Khung, K. Bastari, X.L. Cho, W.A. Yee, S.C.J. Loo, Designing calcium phosphate-based bifunctional nanocapsules with bone-targeting properties, J. Nanoparticle Res. 14 (2012) 911, http://dx.doi.org/10.1007/s11051-012-0911-8.
[134] G. Subramanian, J.G. McAfee, R.J. Blair, F.A. Kallfelz, F.D. Thomas, Technetium-99 m-methylene disphosphonate — a superior agent for skeletal imaging: comparison with other technetium complexes, J. Nucl. Med. 16 (1975) 744–755.
[135] A.I. Brenner, J. Koshy, J. Morey, C. Lin, J. Di Poce, The bone scan, Semin. Nucl. Med. 42 (2012) 11–26, http://dx.doi.org/10.1053/j.semnuclmed.2011.07.005.
[136] E. Palma, J.D.G. Correia, M.P.C. Campello, I. Santos, Bisphosphonates as radionuclide carriers for imaging or systemic therapy, Mol. BioSyst. 7 (2011) 2950, http://dx.doi.org/10.1039/c1mb05242j.
[137] K. Libson, E. Deutsch, B.L. Barnett, Structural characterization of a ^{99}Tc-diphosphonate complex. Implications for the chemistry of ^{99m}Tc skeletal imaging agents, J. Am. Chem. Soc. 102 (1980) 2476–2478.
[138] K. Ogawa, T. Mukai, Y. Inouye, M. Ono, H. Saji, Development of a novel ^{99m}Tc-chelate-conjugated bisphosphonate with high affinity for bone as a bone scintigraphic agent, J. Nucl. Med. 47 (2006) 2042–2047.
[139] E. Palma, B.L. Oliveira, J.D.G. Correia, L. Gano, L. Maria, I.C. Santos, et al., A new bisphosphonate-containing ^{99m}Tc(I) tricarbonyl complex potentially useful as bone-seeking agent: synthesis and biological evaluation, J. Biol. Inorg. Chem. 12 (2007) 667–679, http://dx.doi.org/10.1007/s00775-007-0215-0.
[140] E. Palma, J.D.G. Correia, B.L. Oliveira, L. Gano, I.C. Santos, I. Santos, ^{99m}Tc$(CO)_3$-labeled pamidronate and alendronate for bone imaging, Dalton Trans. 40 (2011) 2787, http://dx.doi.org/10.1039/c0dt01396j.
[141] K. Verbeke, J. Rozenski, B. Cleynhens, H. Vanbilloen, T. de Groot, N. Weyns, et al., Development of a conjugate of ^{99m}Tc-EC with aminomethylenediphosphonate in the search for a bone tracer with fast clearance from soft tissue, Bioconjug. Chem. 13 (2002) 16–22, http://dx.doi.org/10.1021/bc0001600.
[142] L. Liu, G. Zhong, Y. Wei, M. Zhang, X. Wang, Synthesis and biological evaluation of a novel ^{99m}Tc complex of HYNIC-conjugated aminomethylenediphosphonate as a potential bone imaging agent, J. Radioanal. Nucl. Chem. 288 (2011) 467–473, http://dx.doi.org/10.1007/s10967-010-0942-5.
[143] C. Fernandes, S. Monteiro, P. Mendes, L. Gano, F. Marques, S. Casimiro, et al., Biological assessment of novel bisphosphonate-containing ^{99m}Tc/Te-organometallic complexes, J. Organomet. Chem. 760 (2014) 197–204, http://dx.doi.org/10.1016/j.jorganchem.2013.10.038.
[144] N. Chadha, D. Sinha, A.K. Tiwari, K. Chuttani, A.K. Mishra, Synthesis, biological evaluation and molecular docking studies of high-affinity bone targeting N, N′-bis (alendronate) diethylenetriamene-N, N′-triacetic acid: a bifunctional bone scintigraphy agent, Chem. Biol. Drug Des. 82 (2013) 468–476, http://dx.doi.org/10.1111/cbdd.12194.
[145] A. Zaheer, M. Monzur, A.M. De Grand, T.G. Morgan, G. Karsenty, J.V. Frangioni, Optical imaging of hydroxyapatite in the calcified vasculature of transgenic animals, Arterioscler. Thromb. Vasc. Biol. 26 (2006) 1132–1136, http://dx.doi.org/10.1161/01.ATV.0000210016.89991.2a.
[146] K.R. Bhushan, E. Tanaka, J.V. Frangioni, Synthesis of conjugatable bisphosphonates for molecular imaging of large animals, Angew. Chem. Int. Ed. 46 (2007) 7969–7971, http://dx.doi.org/10.1002/anie.200701216.
[147] K.M. Kozloff, R. Weissleder, U. Mahmood, Noninvasive optical detection of bone mineral, J. Bone Miner. Res. 22 (2007) 1208–1216, http://dx.doi.org/10.1359/jbmr.070504.
[148] K.M. Kozloff, L.I. Volakis, J.C. Marini, M.S. Caird, Near-infrared fluorescent probe traces bisphosphonate delivery and retention *in vivo*, J. Bone Miner. Res. 25 (2010) 1748–1758, http://dx.doi.org/10.1002/jbmr.66.
[149] R.J. Tower, G.M. Campbell, M. Müller, O. Will, C.C. Glüer, S. Tiwari, Binding kinetics of a fluorescently labeled bisphosphonate as a tool for dynamic monitoring of bone mineral deposition *in vivo*, J. Bone Miner. Res. 29 (2014) 1993–2003, http://dx.doi.org/10.1002/jbmr.2224.
[150] F.M. Lambers, F. Stuker, C. Weigt, G. Kuhn, K. Koch, F.A. Schulte, et al., Longitudinal *in vivo* imaging of bone formation and resorption using fluorescence molecular tomography, Bone 52 (2013) 587–595, http://dx.doi.org/10.1016/j.bone.2012.11.001.
[151] Y. Zilberman, I. Kallai, Y. Gafni, G. Pelled, S. Kossodo, W. Yared, et al., Fluorescence molecular tomography enables in vivo visualization and quantification of non-union fracture repair induced by genetically engineered mesenchymal stem cells, J. Orthop. Res. 26 (2008) 522–530, http://dx.doi.org/10.1002/jor.20518.
[152] J.L. Figueiredo, C.C. Passerotti, T. Sponholtz, H.T. Nguyen, R. Weissleder, A novel method of imaging calcium urolithiasis using fluorescence, J. Urol. 179 (2008) 1610–1614, http://dx.doi.org/10.1016/j.juro.2007.11.100.
[153] E. Aikawa, M. Nahrendorf, J.L. Figueiredo, F.K. Swirski, T. Shtatland, R.H. Kohler, et al., Osteogenesis associates with inflammation in early-stage atherosclerosis evaluated by molecular imaging *in vivo*, Circulation 116 (2007) 2841–2850, http://dx.doi.org/10.1161/circulationaha.107.732867.
[154] D.D. Felix, J.C. Gore, T.E. Yankeelov, T.E. Peterson, S. Barnes, J. Whisenant, et al., Detection of breast cancer microcalcifications using ^{99m}Tc-MDP SPECT osteosense 750EX FMT imaging, Nucl. Med. Biol. 42 (2015) 269–273, http://dx.doi.org/10.1016/j.nucmedbio.2014.11.010.
[155] F.P. Coxon, K. Thompson, A.J. Roelofs, F.H. Ebetino, M.J. Rogers, Visualizing mineral binding and uptake of bisphosphonate by osteoclasts and non-resorbing cells, Bone 42 (2008) 848–860, http://dx.doi.org/10.1016/j.bone.2007.12.225.
[156] A.J. Roelofs, F.P. Coxon, F.H. Ebetino, M.W. Lundy, Z.J. Henneman, G.H. Nancollas, et al., Fluorescent risedronate analogues reveal bisphosphonate uptake by bone marrow monocytes and localization around osteocytes *in vivo*, J. Bone Miner. Res. 25 (2010) 606–616, http://dx.doi.org/10.1359/jbmr.091009.

[157] C.G. Mick, T. James, J.D. Hill, P. Williams, M. Perry, Molecular imaging in oncology: ^{18}F-sodium fluoride PET imaging of osseous metastatic disease, Am. J. Roentgenol. 203 (2014) 263–271, http://dx.doi.org/10.2214/AJR.13.12158.
[158] A. Elliott, Medical imaging, Nucl. Inst. Methods Phys. Res. A 546 (2005) 1–13, http://dx.doi.org/10.1016/j.nima.2005.03.127.
[159] T. Hamaoka, J.E. Madewell, D.A. Podoloff, G.N. Hortobagyi, N.T. Ueno, Bone imaging in metastatic breast cancer, J. Clin. Oncol. 22 (2004) 2942–2953, http://dx.doi.org/10.1200/JCO.2004.08.181.
[160] M.F. Kircher, J.K. Willmann, Molecular body imaging: MR imaging, CT, and US. Part I. principles, Radiology 263 (2012) 633–643, http://dx.doi.org/10.1148/radiol.12102394.
[161] V. Kubícek, J. Rudovský, J. Kotek, P. Hermann, L. Vander Elst, R.N. Muller, et al., A bisphosphonate monoamide analogue of DOTA: a potential agent for bone targeting, J. Am. Chem. Soc. 127 (2005) 16477–16485, http://dx.doi.org/10.1021/ja054905u.
[162] M. Fellner, R.P. Baum, V. Kubícek, P. Hermann, I. Lukeš, V. Prasad, et al., PET/CT imaging of osteoblastic bone metastases with ^{68}Ga-bisphosphonates: first human study, Eur. J. Nucl. Med. Mol. Imaging 37 (2010) 834-834, http://dx.doi.org/10.1007/s00259-009-1355-y.
[163] M. Fellner, B. Biesalski, N. Bausbacher, V. Kubícek, P. Hermann, F. Rösch, et al., ^{68}Ga-BPAMD: PET-imaging of bone metastases with a generator based positron emitter, Nucl. Med. Biol. 39 (2012) 993–999, http://dx.doi.org/10.1016/j.nucmedbio.2012.04.007.
[164] M. Meckel, M. Fellner, N. Thieme, R. Bergmann, V. Kubicek, F. Rösch, *In vivo* comparison of DOTA based ^{68}Ga-labelled bisphosphonate in non-tumour models, Nucl. Med. Biol. 40 (2013) 823–830, http://dx.doi.org/10.1016/j.nucmedbio.2013.04.012.
[165] K. Suzuki, M. Satake, J. Suwada, S. Oshikiri, H. Ashino, H. Dozono, et al., Synthesis and evaluation of a novel ^{68}Ga-chelate-conjugated bisphosphonate as a bone-seeking agent for PET imaging, Nucl. Med. Biol. 38 (2011) 1011–1018, http://dx.doi.org/10.1016/j.nucmedbio.2011.02.015.
[166] K. Ogawa, K. Takai, H. Kanbara, T. Kiwada, Y. Kitamura, K. Shiba, et al., Preparation and evaluation of a radiogallium complex-conjugated bisphosphonate as a bone scintigraphy agent, Nucl. Med. Biol. 38 (2011) 631–636, http://dx.doi.org/10.1016/j.nucmedbio.2010.12.004.
[167] T. Vitha, V. Kubícek, P. Hermann, L.V. Elst, R.N. Muller, Z.I. Kolar, et al., Lanthanide(III) complexes of bis(phosphonate) monoamide analogues of DOTA: bone-seeking agents for imaging and therapy, J. Med. Chem. 51 (2008) 677–683, http://dx.doi.org/10.1021/jm7012776.
[168] L.E. Cole, T. Vargo-Gogola, R.K. Roeder, Bisphosphonate-functionalized gold nanoparticles for contrast-enhanced X-ray detection of breast microcalcifications, Biomaterials 35 (2014) 2312–2321, http://dx.doi.org/10.1016/j.biomaterials.2013.11.077.
[169] L.E. Cole, T. Vargo-Gogola, R.K. Roeder, Contrast-enhanced X-ray detection of breast microcalcifications in a murine model using targeted gold nanoparticles, ACS Nano 8 (2014) 7486–7496, http://dx.doi.org/10.1021/nn5027802.
[170] L.E. Cole, T. Vargo-Gogola, R.K. Roeder, Contrast-enhanced X-ray detection of microcalcifications in radiographically dense mammary tissues using targeted gold nanoparticles, ACS Nano 9 (2015) 8923–8932, http://dx.doi.org/10.1021/acsnano.5b02749.
[171] L.E. Cole, R.D. Ross, J.M. Tilley, T. Vargo-Gogola, R.K. Roeder, Gold nanoparticles as contrast agents in x-ray imaging and computed tomography, Nanomedicine 10 (2015) 321–341, http://dx.doi.org/10.2217/nnm.14.171.
[172] K. Kouris, N.M. Spyrou, D.F. Jackson, Minimum detectable quantities of elements and compounds in a biological matrix, Nucl. Instrum. Methods. A. 187 (1981) 539–545, http://dx.doi.org/10.1016/0029-554X(81)90386-4.
[173] H. Lusic, M.W. Grinstaff, X-ray-computed tomography contrast agents, Chem. Rev. 113 (2013) 1641–1666, http://dx.doi.org/10.1021/cr200358s.
[174] J.K. Bordoloi, D. Berry, I.U. Khan, K. Sunassee, R.T.M. de Rosales, C. Shanahan, et al., Technetium-99 m and rhenium-188 complexes with one and two pendant bisphosphonate groups for imaging arterial calcification, Dalton Trans. 44 (2015) 4963–4975, http://dx.doi.org/10.1039/c4dt02965h.
[175] H. Hirabayashi, J. Fujisaki, Bone-specific drug delivery systems. Approaches via chemical modification of bone-seeking agents, Clin. Pharmacokinet. 42 (2003) 1319–1330.
[176] R. Torres Martin de Rosales, C. Finucane, J. Foster, S.J. Mather, P.J. Blower, ^{188}Re(CO) 3-dipicolylamine-alendronate: a new bisphosphonate conjugate for the radiotherapy of bone metastases, Bioconjug. Chem. 21 (2010) 811–815, http://dx.doi.org/10.1021/bc100071k.
[177] F.M. Paes, A.N. Serafini, Systemic metabolic radiopharmaceutical therapy in the treatment of metastatic bone pain, Semin. Nucl. Med. 40 (2010) 89–104, http://dx.doi.org/10.1053/j.semnuclmed.2009.10.003.
[178] T. Uehara, Z.L. Jin, K. Ogawa, H. Akizawa, K. Hashimoto, M. Nakayama, et al., Assessment of 186Re chelate-conjugated bisphosphonate for the development of new radiopharmaceuticals for bones, Nucl. Med. Biol. 34 (2007) 79–87, http://dx.doi.org/10.1016/j.nucmedbio.2006.10.001.
[179] K. Ogawa, T. Mukai, Y. Arano, M. Ono, H. Hanaoka, S. Ishino, et al., Development of a rhenium-186-labeled MAG3-conjugated bisphosphonate for the palliation of metastatic bone pain based on the concept of bifunctional radiopharmaceuticals, Bioconjug. Chem. 16 (2005) 751–757, http://dx.doi.org/10.1021/bc040249w.
[180] R.H. Larsen, K.M. Murud, G. Akabani, P. Hoff, O.S. Bruland, M.R. Zalutsky, ^{211}At- and ^{131}I-labeled bisphosphonates with high *in vivo* stability and bone accumulation, J. Nucl. Med. 40 (1999) 1197–1203.
[181] Y. Yang, N. Liu, J. Liao, M. Pu, Y. Liu, M. Wei, et al., Preparation and preliminary evaluation of ^{211}At-labeled amidobisphophonates, J. Radioanal. Nucl. Chem. 283 (2009) 329–335, http://dx.doi.org/10.1007/s10967-009-0384-0.
[182] E. Årstad, P. Hoff, L. Skattebøl, A. Skretting, K. Breistøl, Studies on the synthesis and biological properties of non-carrier-added [^{125}I and ^{131}I]-labeled arylalkylidenebisphosphonates: potent bone-seekers for diagnosis and therapy of malignant osseous lesions, J. Med. Chem. 46 (2003) 3021–3032, http://dx.doi.org/10.1021/jm021107v.
[183] S.A. Gittens, P.I. Kitov, J.R. Matyas, R. Loebenberg, H. Uludag, Impact of tether length on bone mineral affinity of protein-bisphosphonate conjugates, Pharm. Res. 21 (2004) 608–616, http://dx.doi.org/10.1023/b.pham.0000022407.05163.01.
[184] S.A. Gittens, G. Bansal, C. Kucharski, M. Borden, H. Uludag, Imparting mineral affinity to fetuin by bisphosphonate conjugation: a comparison of three bisphosphonate conjugation schemes, Mol. Pharm. 2 (2005) 392–406, http://dx.doi.org/10.1021/mp050017u.
[185] H. Sarin, Physiological upper limits of pore size of different blood capillary types and another perspective on the dual pore theory of microvascular permeability, J. Angiogenes. Res. 2 (2010) 14, http://dx.doi.org/10.1186/2040-2384-2-14.
[186] M.L. Knothe Tate, "Whither flows the fluid in bone?" An osteocyte's perspective, J. Biomech. 36 (2003) 1409–1424, http://dx.doi.org/10.1016/S0021-9290(03)00123-4.
[187] M.K. Danquah, X.A. Zhang, R.I. Mahato, Extravasation of polymeric nanomedicines across tumor vasculature, Adv. Drug Deliv. Rev. 63 (2001) 623–639, http://dx.doi.org/10.1016/j.addr.2010.11.005.
[188] H.S. Choi, W. Liu, P. Misra, E. Tanaka, J.P. Zimmer, B.I. Ipe, M.G. Bawendi, J.V. Frangioni, Renal clearance of nanoparticles, Nat. Biotechnol. 25 (2007) 1165–1170, http://dx.doi.org/10.1038/nbt1340.
[189] S.A. Gittens, K. Bagnall, J.R. Matyas, R. Löbenberg, H. Uludag, Imparting bone mineral affinity to osteogenic proteins through heparin–bisphosphonate conjugates, J. Control. Release 98 (2004) 255–268, http://dx.doi.org/10.1016/j.jconrel.2004.05.001.
[190] G. Bansal, J.E.I. Wright, S. Zhang, R.F. Zernicke, H. Uludag, Imparting mineral affinity to proteins with thiol-labile disulfide linkages, J. Biomed. Mater. Res. 74A (2005) 618–628, http://dx.doi.org/10.1002/jbm.a.30334.
[191] S. Zhang, J.E.I. Wright, G. Bansal, P. Cho, H. Uludag, Cleavage of disulfide-linked fetuin-bisphosphonate conjugates with three physiological thiols, Biomacromolecules 6 (2005) 2800–2808, http://dx.doi.org/10.1021/bm050273s.
[192] S.A. Gittens, J.R. Matyas, R.F. Zernicke, H. Uludag, Imparting bone affinity to glycoproteins through the conjugation of bisphosphonates, Pharm. Res. 20 (2003) 978–987, http://dx.doi.org/10.1023/a:1024459033306.